A Conserved Metabolic Network Orchestrates Melanin-Dependent Titan Cell Formation in *Cryptococcus neoformans*

Pallavi S Phatak[1,2], Sudharsan Mathivathanan[1], Dhrumi Shah[1,2], Ishvarya Suresh[1], Mary Shejo[1], Santosh Kumar Das[1,2] and Sriram Varahan[1,2#]

Affiliations:

[1]CSIR-Centre for Cellular and Molecular Biology, Uppal Road, Hyderabad 500007, India.

[2]Academy of Scientific and Innovative Research (AcSIR), Ghaziabad- 201002, India.

 # - Corresponding Author:

Dr. Sriram Varahan

Senior Scientist

CSIR-Centre for Cellular and Molecular Biology (CCMB)

Email: sriram.ccmb@csir.res.in

Abstract

Cryptococcus neoformans is an opportunistic fungal pathogen that primarily causes pulmonary infections, with the potential to cause life-threatening infections including meningoencephalitis in immunocompromised individuals. Key virulence factors including polysaccharide capsule and melanin, facilitate immune evasion and tissue invasion in the host. Recently, titan cell formation has been defined as another important virulence factor of *C. neoformans* and plays a pivotal role in disease progression. The cyclic AMP–protein kinase A (cAMP-PKA) pathway in *C. neoformans* has been shown to be an important regulator of virulence-associated processes, including capsule formation, melanin biosynthesis and titan cell formation. However, the upstream signals, critical for the activation of cAMP-PKA pathway in the context of titan cell formation remain poorly understood. In this study, we demonstrate that the central carbon metabolic pathway, glycolysis, is critical for cAMP-dependent titan cell formation. Pharmacological and genetic perturbation of glycolysis significantly attenuated titan cell formation. Remarkably, exogenous addition of cAMP completely reversed the titan cell defects, observed during glycolysis perturbation. Interestingly, melanin deficient strains exhibited a significant attenuation in titan cell formation establishing a novel link between dimorphic switching and melanin biosynthesis in *C. neoformans*. These findings establish a novel regulatory axis wherein central carbon metabolism orchestrates morphogenetic switching in *C. neoformans* by regulating the activity of the well-conserved cAMP-PKA pathway. We also demonstrate, for the first time, that melanin biosynthesis which is under the regulatory control of cAMP-PKA pathway, is critical for titan cell formation, providing new insights into the metabolic control of *C. neoformans* dimorphism.

Summary

A leading opportunistic fungal pathogen, *Cryptococcus neoformans* possess a significant threat to human health. Titan cell formation is one of the established virulence factors of *C. neoformans*. However, the mechanisms underlying the regulation of titan cell formation remains largely uncharacterized. Our study demonstrates that glycolysis regulates titan cell formation in a cAMP-PKA pathway dependent manner and melanin biosynthesis, which is under the direct regulatory control of cAMP-PKA pathway, is critical for titan cell formation. This study offers crucial insights into the metabolic regulation of dimorphic transitions in the human fungal pathogen, *C. neoformans*.

Key words: *Cryptococcus neoformans*, Capsule, Melanin, Titan cell formation, cAMP-PKA pathway, Glycolysis

Introduction

Cryptococcus neoformans is an opportunistic fungal pathogen that significantly impacts global public health, and causes life-threatening infections especially in immunocompromised individuals (Zhao et al. 2023). This pathogen is responsible for causing cryptococcosis that primarily manifests as a pulmonary infection but can disseminate to cause severe meningoencephalitis (Rajasingham et al. 2017; Chen et al. 2018). With an estimated 220,000 cases of cryptococcal meningitis occurring annually worldwide, resulting in approximately 180,000 deaths, *C. neoformans* has been designated as a critical priority fungal pathogen by the World Health Organization (WHO) (Rajasingham et al. 2017; Zhao et al. 2023). The pathogenicity of *C. neoformans* is attributed to several well-characterized virulence factors that facilitate immune evasion and tissue invasion in the host (Zaragoza 2019). The polysaccharide capsule, composed primarily of glucuronoxylomannan and galactoxylomannan, serves as a major virulence determinant by inhibiting phagocytosis and modulating the host immune response in favour of *C. neoformans* survival (Zaragoza et al. 2009; O'Meara and Andrew Alspaugh 2012). Additionally, melanin production through laccase-mediated oxidation of phenolic compounds, provides protection against oxidative stress and antimicrobial peptides, contributing to *C. neoformans* survival within the host (Nosanchuk and Casadevall 2003; Eisenman and Casadevall 2012). In recent years, morphological plasticity has emerged as another critical virulence mechanism in *C. neoformans* (Okagaki et al. 2010). While the organism typically exists as a budding yeast with cells ranging from 5-7μm in diameter, several studies have shown that, upon host entry, *C. neoformans* undergoes a dramatic morphological transition resulting in the formation of unusually large cells known as 'Titan cells' (Cruickshank et al. 1973; Crabtree et al. 2012; Zhou and Ballou 2018). Titan cells are defined as enlarged cells with a diameter of ≥10μm (with some cells reaching sizes up to ~100μm) (Zhou and Ballou 2018). Several studies have shown that titan cells are resistant to phagocytosis as well as oxidative and nitrosative stresses within the host (Crabtree et al. 2012; Okagaki and Nielsen 2012; García-Rodas et al. 2019). Similarly, *in vivo* studies suggest that titan cells play a pivotal role in cryptococcal dissemination and disease progression within the host (Okagaki et al. 2010; García-Barbazán et al. 2016). Apart from increased cell size, titan cells exhibit a high degree of polyploidy, a significantly thickened cell wall and capsule with an altered compositions (Mukaremera et al. 2018; Zhou and Ballou 2018; García-Rodas et al. 2019). Titan cells also exhibit significant variations in homeostatic cellular processes compared to typical yeast cells, including alterations in cell cycle progression with an extended G2 phase and G2/M arrest (Zaragoza and Nielsen 2013; Altamirano et al. 2021).

Cyclic adenosine-3',5'-monophosphate-protein kinase A (cAMP-PKA) pathway is a highly conserved eukaryotic signalling cascade that regulates diverse cellular processes, including stress responses, metabolic adaptation, and morphogenetic transitions in various fungal species (D'Souza and Heitman 2001; Pukkila-Worley and Alspaugh 2004; Caza and Kronstad 2019). cAMP-PKA pathway is highly responsive to nutrient availability, specifically glucose levels and glycolytic flux and regulates various cellular processes in response to these metabolic cues (Busti et al. 2010; Caza and Kronstad 2019). In *C. neoformans*, cAMP-PKA pathway has emerged as a central regulator of key virulence factors including melanin, capsule and titan cell formation (Alspaugh et al. 1997; D'Souza et al. 2001; Caza and Kronstad 2019; Yu et al. 2025). Deletion strains that lack the genes encoding various cAMP-PKA

pathway components, such as Cac1 (adenylate cyclase) or Pka1 (catalytic subunit of PKA), are unable to undergo titanization both *in vitro* and *in vivo* (D'Souza et al. 2001; Zaragoza et al. 2010; Hommel et al. 2018; Trevijano-Contador et al. 2018), while deletion strains that lack the Pka regulatory subunit, Pkr1 exhibit increased titanization (Choi et al. 2012; Hommel et al. 2018). Recently, a series of landmark studies have established that *in vitro* titanization assays results in the reproducible generation of titan cells that faithfully recapitulate the various biological signatures of titan cells that are generated *in vivo* (Dambuza et al. 2018; Hommel et al. 2018; Trevijano-Contador et al. 2018). Interestingly, one of these studies showed that several glycolytic genes were upregulated under *in vitro* titan cell inducing conditions suggesting a possible link between central carbon metabolism and titan cell formation (Trevijano-Contador et al. 2018). However, the precise role of glycolysis in the context of titan cell formation remains unexplored. Interestingly, the link between glycolysis and cAMP-PKA signalling has been well-established in the model fungi *Saccharomyces cerevisiae* (Busti et al. 2010; Peeters et al. 2017). The conservation of this regulatory link in other fungi, specifically the human pathogen *C. neoformans*, has not been completely explored. Given the fact that cAMP-PKA pathway is an important regulator of titan cell formation (Pukkila-Worley and Alspaugh 2004; Okagaki et al. 2011; Caza and Kronstad 2019), we hypothesized that glycolysis flux could be one of the upstream signals critical for the activation cAMP-PKA pathway, in the context of titan cell formation.

Our findings reveal a critical role for glycolysis, in regulating titan cell formation in *C. neoformans*, in a cAMP-PKA dependent manner. We demonstrate that perturbation of glycolysis using pharmacological inhibitors or pertinent knockout strains, significantly attenuated titan cell formation. Furthermore, we observed that perturbation of glycolysis negatively affects the intracellular levels of cAMP and subsequently, the expression of cAMP-PKA pathway regulated genes involved in capsule formation and melanin biosynthesis specifically under titan cell inducing conditions (Pukkila-Worley et al. 2005; Cramer et al. 2006). Remarkably, the addition of exogenous cAMP reversed the defects in titan cell formation caused by glycolysis perturbation, thereby establishing a novel regulatory link between glycolysis and the cAMP–PKA pathway in *C. neoformans*. Additionally, for the first time, our study demonstrates a direct role of melanin biosynthesis during titan cell formation suggesting a possible interdependency between these two well-established virulence factors. Taken together, these findings elucidate the role of a conserved metabolic pathway in coordinating fungal morphogenesis *via* a well-conserved signaling module in the fungal pathogen *C. neoformans*.

Results

Perturbation of Glycolysis Attenuates Titan Cell Formation in *C. neoformans*:

Among a range of different morphotypes exhibited by *C. neoformans* (Stempinski et al. 2023; Brown and Ballou 2024), titan cells, defined as cells with a diameter of ≥10μm, represent an important virulence lifestyle critical for host pathogenesis (Okagaki et al. 2010; Crabtree et al. 2012). Previous studies have shown that despite their increased size, titan cells are metabolically active and exhibit significant variations in a variety of homeostatic cellular processes compared to the yeast cells of *C. neoformans* (García-Barbazán et al. 2024). Titan cell formation is associated with altered cell cycle wherein cells are observed to have extended

182 G2 phase and G2/M arrest (Altamirano et al. 2021). Titan cells also possess a thicker cell wall
183 and capsule with a significantly altered composition, compared to the yeast cells (cells with a
184 diameter of 5-7μm) (Hommel et al. 2018; Mukaremera et al. 2018). Several studies have
185 suggested a strong interdependency between cellular metabolism and changes in cell size,
186 ploidy or cell envelope composition (Kalucka et al. 2015; Sachla and Helmann 2021; Cadart
187 and Heald 2022; Diehl et al. 2024). Importantly, glycolysis plays a central role in the generation
188 of precursors needed for the biosynthesis of various cell wall sugars (glucans, mannan,
189 glucosamine, xylose, galactose etc.), nucleic acids, and lipids (Kierans and Taylor 2024).
190 Similarly, various studies have demonstrated a critical role for glycolysis in the regulation of
191 cell cycle progression across different species (Kalucka et al. 2015; Diehl et al. 2024). Despite
192 the fact that titan cell formation in *C. neoformans* exhibits all the aforesaid changes including
193 increase in cell size, alteration in cell cycle progression and variation in cell envelope
194 architecture, the role of central carbon metabolic pathways including glycolysis has not been
195 explored in this context.
196
197 To investigate the functional requirement of glycolysis in titan cell formation, we tested the
198 ability of *C. neoformans* to undergo titanization, using the previously established *in vitro* titan
199 cell assay (Trevijano-Contador et al. 2018). Briefly, wild-type *C. neoformans* strain H99 was
200 cultured in Titan Cell Medium (TCM) in the presence and absence of sub-inhibitory
201 concentrations of well-established glycolysis inhibitors, 2-Deoxy-D-glucose (2DG) and sodium
202 citrate (NaCi), which target the early and rate-limiting steps of the glycolysis pathway and titan
203 cell formation was subsequently assessed (Trevijano-Contador et al. 2018) (Fig. 1A). 2DG, a
204 glucose analogue, acts as a competitive inhibitor of hexokinase (Hxk) and phosphoglucose
205 isomerase (Pgi), thereby perturbing glycolysis at its initial steps (Cramer and Woodward
206 1952). Similarly, NaCi, interferes with the activity of phosphofructokinase (Pfk), which is a key
207 rate-limiting enzyme in the glycolysis pathway (Yoshino and Murakami 1982). Previous studies
208 have shown that when *C. neoformans* grown in titan cell inducing medium, a heterogeneous
209 population of cells emerge wherein the cell size ranges from 2μm to ≥10μm, and the cells that
210 2-3μm in diameter have been reported as titanides (Feldmesser et al. 2001; Dambuza et al.
211 2018). Consistent with the literature, we also observed a heterogeneous population of cells
212 including previously defined titanides (2-3μm), regular size yeast cells (5-7μm), cells between
213 7μm to 10μm and cells ≥10μm. In our study, we focused on the cells that are ≥10μm,
214 designated as titan cells and the percentage of titan cells were quantified as the ratio of titan
215 cells (≥10μm) to the total number of cells. Our data clearly demonstrates that sub-inhibitory
216 concentrations of 2DG and NaCi significantly attenuate the ability of *C. neoformans* to undergo
217 titan cell formation (Fig. 1B and C; Fig. S1A). To rule out the possibility that the phenotype we
218 observed is due to a general growth defect, we assessed the viability of *C. neoformans*, under
219 titan cell inducing conditions in the presence of glycolysis inhibitors using CFU (Colony
220 Forming Units) quantification. Our results clearly demonstrate that the reduction in titan cell
221 formation is not due to a general growth defect, as presence of sub-inhibitory concentrations
222 of 2DG and NaCi did not affect the viability of the wild-type strain (Fig. 1D). Titan cells are
223 known to have a thicker and more complex capsule structure compared to the capsule of yeast
224 cells. Additionally, in the field, titan cells have been defined by their cell size either including
225 or excluding the capsule (García-Rodas et al. 2019). Increased capsule expansion is thought
226 to be an important morphological hallmark of titan cells, and given this, we wanted to assess
227 whether the perturbation of glycolysis affects titan cell associated capsule thickness, and
228 consequently, overall cell size including the capsule. In order to do this, wild-type cells were
229 grown in TCM in the presence and absence of sub-inhibitory concentrations of glycolysis

230 inhibitors and capsule was visualized using India ink staining and capsule thickness was
231 quantified. Our data shows that the addition of 2DG or NaCi resulted in a significant reduction
232 in overall capsule thickness and total cell diameter (Fig. 1E and F; Fig. S1B). This
233 demonstrates that the perturbation of glycolysis disrupts titan cell associated capsule
234 expansion.
235
236 Given that, 2DG and NaCi exhibited a strong inhibitory effect on titan cell formation, we wanted
237 to corroborate these observations by using pertinent genetic knockout strains that are
238 compromised in their ability to metabolize glucose *via* glycolysis (Price et al. 2011). In order
239 to do this, we tested the ability of knockout strains which lack the genes that encode for
240 enzymes that are involved in the glycolysis pathway including, Hxk2 (Hexokinase 2) and Pyk1
241 (Pyruvate kinase 1) (Price et al. 2011) (Fig. 2A). In *C. neoformans*, *hxk2* encodes for the
242 enzyme that catalyses the phosphorylation of glucose to glucose-6-phosphate (Idnurm et al.
243 2007), while *pyk1* encodes for the enzyme responsible for converting phosphoenolpyruvate to
244 pyruvate (Price et al. 2011). Briefly, *hxk2*Δ and *pyk1*Δ (*hxk2*Δ refers to the *hxk2* knockout
245 strain and *pyk1*Δ refers to the *pyk1* knockout strain) along with the wild-type were cultured in
246 TCM and incubated at 37 °C under 5% CO_2 for 72 hours. Cells were imaged using bright field
247 microscopy, and percentage of titan cells was quantified as the ratio of titan cells (≥10µm) to
248 the total number of cells. Our result demonstrates that the deletion of *hxk2* and *pyk1* resulted
249 in a significant reduction in titan cell formation, compared to the wild-type strain (Fig. 2B and
250 C; Fig. S2A). To rule out the possibility that the phenotype we observed is due to a general
251 growth defect, we performed CFU assay using the wild-type and knockout strains (*hxk2*Δ and
252 *pyk1*Δ*)* grown in titan cell inducing conditions. Our data suggests that the reduction in titan cell
253 formation is not due to a general growth defect as there was no significant difference in the
254 viability of the wild-type and mutants grown under titan cell inducing conditions. (Fig. 2D).
255 Given that the perturbation of glycolysis using 2DG or NaCi leads to reduced titan cell
256 associated capsule thickness in the wild-type, we wanted to corroborate these observations
257 by using pertinent genetic knockout strains (*hxk2*Δ and *pyk1*Δ*)* that are compromised in their
258 ability to undergo glycolysis. In order to do this, glycolysis knockout strains including, *hxk2*Δ
259 and *pyk1*Δ along with the wild-type were cultured in TCM and capsule was visualized using
260 India ink staining and capsule thickness was measured. Bright field microscopy revealed that
261 glycolysis knockout strains exhibited a significant decrease in capsule thickness compared to
262 the wild-type strain (Fig. 2E and F; Fig. S2B).
263
264 To confirm that the defects observed in titan cell formation, in the glycolysis mutants (*hxk2*Δ
265 and *pyk1*Δ), were not due to any off-target integrations, chromosomal deletions/duplications,
266 and tandem integrations caused by the transformation procedure, we validated our results
267 using complemented strains for these mutants. Our results demonstrated that the
268 complemented strains, *hxk2*Δ + *HXK2* and *pyk1*Δ + *PYK1* exhibited complete rescue of the
269 titanization defects exhibited by the mutants, *hxk2*Δ and *pyk1*Δ (Fig. 2G; Fig. S2C). These
270 complementation strains were also tested for titan cell associated capsule formation and total
271 cell size, using India ink staining. As shown in the Fig. 2H, complemented strains *hxk2*Δ +
272 *HXK2* and *pyk1*Δ + *PYK1* exhibited complete rescue of the defects observed in titan cell
273 associated capsule formation in the glycolysis mutants *hxk2*Δ and *pyk1*Δ (Fig. S2D). Taken
274 together, our results clearly demonstrate that the ability of *C. neoformans* to efficiently
275 metabolize glucose *via* glycolysis is critical for titan cell formation.
276

Active Glycolysis is Critical for cAMP-PKA Signalling in Titan Cell Inducing Conditions:

Our data clearly demonstrates that the perturbation of glycolysis using inhibitors or pertinent knockout strains attenuates titan cell formation in *C. neoformans*. Several studies have established that fungi use different pathways to sense nutrient availability and modulate their metabolic state in order to regulate growth and proliferation (Bahn et al. 2007; Yuan et al. 2013). For example, glucose availability and the glycolytic flux is sensed by the conserved signalling pathway, cyclic-AMP-Protein Kinase A (cAMP-PKA) pathway in *S. cerevisiae* and it has been shown that active glycolysis is critical for the full activation of this pathway (Busti et al. 2010; Peeters et al. 2017). In *C. neoformans,* cAMP-PKA pathway is known to play an important role in host pathogenesis by regulating three critical virulence factors including capsule formation, melanin biosynthesis and titan cell formation (Hicks et al. 2004; Caza and Kronstad 2019; Mahmood et al. 2024). Given the fundamental and highly conserved nature of both glycolysis and the cAMP-PKA pathway across various fungal species (Fuller and Rhodes 2012; Caza and Kronstad 2019; Yu and Rollins 2022), we hypothesized that the glycolysis-dependent regulation of titan cell formation is mediated through the cAMP-PKA pathway. To test this hypothesis, we sought to evaluate the activity of cAMP-PKA pathway at two distinct levels, during glycolysis perturbation in titan cell inducing conditions. First, we quantified the intracellular levels of cAMP, in *C. neoformans* wild-type and glycolysis mutants. Second, we analysed the gene expression of known downstream effectors of cAMP-PKA pathway in *C. neoformans* (Pukkila-Worley et al. 2005; Cramer et al. 2006), in glycolysis mutants, compared to the wild-type, under titan cell inducing conditions.

In order to quantify the intracellular levels of cAMP in the wild-type and glycolysis mutants, these strains were grown in TCM for 24 hours, and intracellular cAMP levels were measured using the cAMP-Glo assay kit (#V1501 - Promega). Our results demonstrate that intracellular cAMP levels were consistently higher in the wild-type strain as compared to the glycolysis mutants, including *hxk2*Δ and *pyk1*Δ under the tested conditions. This suggests that perturbation of glycolysis negatively influences the intracellular levels of cAMP, leading to the reduced activation of cAMP-PKA cascade (Fig. 3C). In order to confirm that the perturbation of glycolysis leads to downregulation of the cAMP-PKA pathway, in titan cell inducing conditions, we measured the expression of a known downstream target, *cap10*. In *C. neoformans*, Cap10 has been shown to be involved in capsule biosynthesis (Fig. 3A) (Pukkila-Worley et al. 2005). To determine the relative expression of *cap10* glycolysis knockout strains including *hxk2*Δ and *pyk1*Δ along with the wild-type strain were cultured in titan cell inducing conditions for 72 hours, following which total RNA was extracted and gene expression levels were quantified using RT-qPCR. Our data shows that the expression of *cap10* was significantly downregulated in *hxk2*Δ and *pyk1*Δ as compared to wild-type strain (Fig 3B). Similarly, we monitored the expression of other cAMP-PKA downstream targets, *lac1* and *lac2* (Pukkila-Worley et al. 2005; Yu et al. 2025) in glycolysis knockout strains including, *hxk2*Δ and *pyk1*Δ along with the wild-type strain in titan cell inducing conditions. In *C. neoformans*, both *lac1* and *lac2* encodes for the laccase enzyme which catalyses an important step in melanin biosynthesis (Pukkila-Worley et al. 2005) (Fig. 3A). Briefly, glycolysis knockout strains including *hxk2*Δ and *pyk1*Δ*,* along with the wild-type strain were cultured in titan cell inducing conditions for 72 hours, following which total RNA was extracted and gene expression levels

were quantified using RT-qPCR. Our results indicate that both *lac1* and *lac2* were significantly downregulated in *hxk2*Δ and *pyk1*Δ compared to wild-type strain (Fig. 3B).

These findings indicate a clear regulatory link between glycolysis and the cAMP-PKA pathway during titan cell formation in *C. neoformans*. While it is established that cAMP levels in *C. neoformans* is linked to glucose availability, the specific extracellular glucose receptors and underlying mechanistic details remain undiscovered (Hommel et al. 2018). Our data demonstrate a positive correlation between glycolysis and the cAMP-PKA pathway specifically under titan cell inducing conditions. To determine if this connection is conserved under general nutrient-rich growth environments, we quantified cAMP levels and the expression of key cAMP-PKA target genes in both wild-type and glycolysis-deficient mutants grown in standard YPD medium at 37 °C (Fig. 3D). Interestingly, we observed no significant differences in cAMP levels or target gene expression between the mutants and the wild-type strain under these standard laboratory growth conditions (Fig. 3D and E). This suggests that the regulatory influence of glycolysis on the cAMP-PKA pathway exists specifically under titan cell inducing conditions. Overall, these results indicate that the perturbation of glycolysis results in reduced intracellular levels of cAMP which in turn negatively influences the expression of genes which are regulated by the cAMP-PKA pathway under titan cell inducing condition. This suggests that active glycolytic flux might be important for the robust activation of the cAMP-PKA pathway and its downstream regulon, only during titan cell formation and not during general growth in nutrient-rich medium.

Glycolysis Orchestrates Titan Cell Formation in a cAMP-PKA Dependent Manner:

Our RT-qPCR results clearly demonstrated that the perturbation of glycolysis negatively affects several downstream targets of cAMP-PKA pathway under titan cell inducing conditions. Moreover, we observed significant reduction in intracellular cAMP levels in glycolysis mutants under titan cell inducing treatment. Given the central role of cAMP-PKA pathway in titan cell formation, the observed defects in titanization under glycolysis perturbation might be attributable to glycolysis-mediated reduction in cAMP levels and henceforth downregulation of cAMP-PKA pathway. To test this hypothesis, we performed cAMP-add back assays wherein glycolysis knockout strains including *hxk2*Δ and *pyk1*Δ along with wild-type strain were cultured in TCM with and without the exogenous supplementation of cAMP (10mM) and incubated under titan cell inducing conditions. Cells were imaged using bright field microscopy, and percentage of titan cells was quantified as the ratio of titan cells (≥10μm) to the total number of cells. Remarkably, exogenous supplementation of cAMP significantly rescued the titan cell formation defect observed in *hxk2*Δ and *pyk1*Δ strains (Fig. 4A and C; Fig. S3A). The percentage of titan cells were significantly higher in the cAMP treated *hxk2*Δ and *pyk1*Δ strains compared to the untreated controls, reaching levels comparable to the wild-type strain (Fig. 4A and C; Fig. S3A).

cAMP-PKA pathway is a known positive regulator of capsule formation in *C. neoformans* (Leadsham and Gourlay 2010). Given that exogenous supplementation of cAMP significantly rescued titan cell formation defects observed in the glycolysis knockout strains, we wanted to assess whether cAMP add-back rescues titan cell associated capsule thickness, and consequently, overall cell size including the capsule. In order to do this, glycolysis knockout

370 strains including *hxk2*Δ and *pyk1*Δ along with the wild-type strain were cultured in TCM with
371 and without exogenous supplementation of cAMP (10mM) and incubated under titan cell
372 inducing conditions. Capsule was visualized using India ink staining and capsule thickness
373 was measured. Our data demonstrates that the exogenous supplementation of cAMP leads
374 to significant increase in capsule thickness of *hxk2*Δ and *pyk1*Δ strains compared to the
375 untreated cultures of *hxk2*Δ and *pyk1*Δ strains, reaching levels comparable to the wild-type
376 strain (Fig. 4B and D; Fig. S3B). Collectively, our results indicate that glycolysis regulates titan
377 cell formation through the activation of the cAMP-PKA pathway.
378
379 **Melanin Biosynthesis is Critical for Titan Cell Formation in *C. neoformans*:**
380
381 Our RT-qPCR results demonstrated that under titan cell inducing conditions, functional
382 glycolysis is essential for the expression of genes involved in melanin biosynthesis including
383 *lac1* and *lac2*, in a cAMP-PKA pathway dependent manner. Although in *C. neoformans,*
384 melanin is a known virulence factor that contributes towards host pathogenesis, its direct
385 involvement in titan cell formation remains unexplored (Zaragoza 2019). In order to determine
386 whether the downregulation of genes involved in melanin biosynthesis, directly contributes
387 towards the attenuation of titan cell formation under glycolysis perturbation, we tested the
388 ability of a knockout strain (*lac2*Δ) which is impaired in melanin biosynthesis (Pukkila-Worley
389 et al. 2005), to undergo titan cell formation. To confirm that the phenotype observed in the
390 melanin deficient strain (*lac2*Δ), were not due to any off-target integrations, chromosomal
391 deletions/duplications, and tandem integrations caused by the transformation procedure, we
392 included a complementation strain (*lac2*Δ + LAC2) in our assays. Briefly, *lac2*Δ and *lac2*Δ +
393 LAC2 strains along with the wild-type strain were cultured in TCM and incubated at 37 °C
394 under 5% CO_2, for 72 hours. Cells were imaged using bright field microscopy, and percentage
395 of titan cells was quantified as the ratio of titan cells (≥10μm) to the total number of cells. Our
396 results demonstrate that the deletion of *lac2*Δ resulted in a significant reduction in titan cell
397 formation, compared to the wild-type strain (Fig. 5A; Fig. S4A), while the complemented strain
398 exhibited titanization comparable to the wild type strain. In *C. neoformans*, laccase activity is
399 encoded by two paralogs, *lac1* and *lac2* (Pukkila-Worley et al. 2005). Since *lac1* remains
400 functional in *lac2Δ* mutants, we further evaluated titan cell formation in a double-deletion strain
401 (*lac1*Δ*lac2*Δ) which is completely deficient in laccase production. The double deletion strain,
402 *lac1*Δ*lac2*Δ resulted in significant reduction in titan cell formation (Fig. 5A; Fig. S4A) similar to
403 the *lac2*Δ strain. As a confirmation, the aforementioned strains were tested for their ability to
404 synthesize melanin, in melanin inducing medium. As shown in the Fig. 5B, deletion strains
405 *lac2*Δ and *lac1*Δ*lac2*Δ were defective in melanin biosynthesis after incubation for 36 hours in
406 melanin inducing medium.
407
408 Additionally, we measured titan cell associated capsule formation for *lac2*Δ, its complemented
409 strain, *lac2*Δ + LAC2 and double knockout strain *lac1*Δ*lac2*Δ, in titan cell inducing conditions,
410 similar to our previous experiments. Strains, *lac2*Δ, *lac2*Δ + LAC2, *lac1*Δ*lac2*Δ along with the
411 wild-type strain were cultured in TCM and incubated at 37 °C under 5% CO_2 for 72 hours.
412 Capsule was visualized using India ink staining and capsule thickness was measured. Bright
413 field microscopy revealed that *lac2*Δ exhibited a significant decrease in total cell diameter
414 which includes both the cell body and the surrounding capsule relative to the wild-type strain
415 (Fig. 5C and D; Fig. S4B). These findings, for the first time, establish a direct role for melanin

416 biosynthesis during titan cell formation in *C. neoformans*, highlighting the regulatory
417 interdependencies of these virulence factors.
418
419 ## Discussion
420
421 Our findings provide compelling evidence for a conserved regulatory axis that links central
422 carbon metabolism, specifically glycolysis and cAMP-PKA pathway in the regulation of titan
423 cell formation in *C. neoformans.* Even though several studies have demonstrated that cAMP-
424 PKA pathway is critical for titan cell formation (Zaragoza et al. 2010; Okagaki et al. 2011; Zhou
425 and Ballou 2018; Caza and Kronstad 2019), the upstream signals that are required for the
426 activation of this pathway during titan cell formation remains poorly understood. Titan cells
427 exhibit dramatically altered cellular and morphological changes compared to the yeast
428 morphotype and these include increase in cell size, polyploidy resulting from
429 endoreduplication and thicker cellular envelope (cell wall and polysaccharide capsule) with
430 altered composition (Zhou and Ballou 2018; García-Rodas et al. 2019). Importantly, glycolysis
431 plays a critical role in generating various precursors required for cell wall and capsule
432 biosynthesis, and the role of glycolysis in regulating cell size and cell cycle progression in
433 various organisms including multiple fungal species is well established (Cadart and Heald
434 2022; Diehl et al. 2024; Kierans and Taylor 2024). Furthermore, glycolysis has been recently
435 implicated in the regulation of fungal morphogenesis, particularly in *S. cerevisiae* and *Candida*
436 *albicans* (Shah et al. 2026). A recent study that reported the successful generation of *in vitro*
437 titan cells which are remarkably similar to the titan cells that are formed *in vivo*, during *C.*
438 *neoformans* infections, demonstrated that *in vitro* titan cells have increased expression of
439 several glycolytic genes (Trevijano-Contador et al. 2018). Given these observations, we
440 hypothesized that glycolysis might play an important role in the regulation of titan cell formation
441 in *C. neoformans*. Our results clearly demonstrated that the inhibition of glycolysis with sub-
442 inhibitory concentrations of 2DG or NaCi significantly reduced titan cell formation, providing
443 strong evidence for the metabolic dependency of this morphogenetic process. These findings
444 were further supported by the results from titan cell assays using pertinent glycolysis deletion
445 strains, wherein *hxk2*Δ (*hxk2*Δ refers to the *hxk2* deletion strain) and *pyk1*Δ (*pyk1*Δ refers to
446 the *pyk1* deletion strain) showed a substantial reduction in titan cell formation compared to the
447 wild-type.
448
449 The cAMP-PKA pathway is a well-established sensor of nutrient availability, particularly
450 glucose, across various fungal species (Pukkila-Worley and Alspaugh 2004; Busti et al. 2010).
451 In *Saccharomyces cerevisiae*, this pathway integrates extracellular glucose levels and
452 intracellular metabolic flux through distinct mechanisms. The membrane-bound G-protein
453 coupled receptor (GPCR), Gpr1, responds to ambient glucose concentrations, to modulate
454 cAMP synthesis. Concurrently, the glycolysis intermediate fructose-1,6-bisphosphate
455 regulates cAMP synthesis in a Ras1-dependent manner. (Xue et al. 1998; Pukkila-Worley and
456 Alspaugh 2004; Busti et al. 2010; Peeters et al. 2017). In *C. neoformans*, intracellular cAMP
457 levels increases in response to glucose availability, though the underlying mechanisms remain
458 unknown (Xue et al. 2006). While the G-protein coupled receptor Gpr4 shares significant
459 homology with the *S. cerevisiae* glucose sensor Gpr1, it primarily responds to methionine
460 levels to regulate the cAMP-PKA pathway (Xue et al. 2006). Consequently, the specific
461 extracellular receptors and the precise molecular mechanisms governing glucose mediated
462 regulation of this pathway in *C. neoformans* are yet to be identified (Pukkila-Worley and

463 Alspaugh 2004). Given the nutrient responsive nature of cAMP-PKA pathway and the fact that
464 this cascade is central for the regulation of titan cell formation, we hypothesised that the effect
465 of glycolysis perturbation on titan cell formation could be mediated through the activation of
466 cAMP-PKA pathway. Supporting our hypothesis, we observed significant reduction in the
467 intracellular cAMP levels, in the glycolysis mutants, compared to the wild-type, in titan cell
468 inducing conditions. The significantly reduced intracellular levels of cAMP, explains the
469 reduced activity of the cAMP-PKA pathway in the glycolysis mutants (*hxk2*Δ and *pyk1*Δ). This
470 was demonstrated by the transcriptional downregulation of cAMP-PKA pathway target genes
471 (*cap10, lac1,* and *lac2*) in pertinent glycolysis knockout strains including *hxk2*Δ and *pyk1*Δ
472 compared to the wild-type strain, confirming our aforesaid hypothesis that perturbation of
473 glycolysis leads to reduced intracellular levels of cAMP which in turn results in downregulation
474 of the cAMP-PKA pathway during titan cell formation. Remarkably, exogenous
475 supplementation of cAMP rescues titan cell formation defects exhibited by glycolysis knockout
476 strains (*hxk2*Δ and *pyk1*Δ*)*, strongly suggesting that glycolysis functions upstream of cAMP-
477 PKA activation, thereby establishing a metabolic checkpoint for this morphogenetic transition
478 (Fig. 6). Notably, this regulatory coupling appears to be context-dependent, as we observed
479 no significant change in cAMP levels or the expression of downstream target genes regulated
480 by the cAMP-PKA pathway, when mutants were cultured under standard nutrient-rich (YPD)
481 conditions. These findings suggest that the metabolic crosstalk between glycolysis and the
482 cAMP-PKA pathway in *C. neoformans* is uniquely required during titan cell formation. The
483 cAMP-PKA pathway is a widely recognized central regulator of cell growth. It plays a key role
484 in influencing essential cellular processes, including ribosome biogenesis, mitochondrial
485 biogenesis, and the regulation of cell wall biosynthesis (Hu et al. 2007; Yoboue et al. 2012;
486 Guerra et al. 2022). Given that, titan cells exhibit characteristic features of increased cell size
487 and altered cell wall compositions, our finding that glycolysis-mediated activation of cAMP-
488 PKA pathway is critical for titan cell formation, is highly significant and further studies are
489 required to delineate the underlying mechanism.
490
491 The cAMP-PKA signaling pathway is a well-established central regulator of three primary
492 virulence factors in *C. neoformans,* including capsule, melanin, and titan cell formation
493 (Zaragoza 2019). While previous research has established that capsule deficient mutants are
494 defective in titanization (Hommel et al. 2018), the direct involvement of melanin biosynthesis
495 in titan cell formation has remained unexplored. To address this knowledge gap and determine
496 if impaired melanization contributes to titan cell formation, we evaluated the titanization ability
497 of melanin deficient strains (*lac2*Δ and *lac1*Δ*lac2*Δ) (Pukkila-Worley et al. 2005). Interestingly,
498 our results demonstrate that the deletion of *lac* genes results in a significant reduction in titan
499 cell formation. These findings, for the first time, establish a direct role for melanin biosynthesis
500 in titan cell formation in *C. neoformans*. Melanin could contribute towards titan cell formation
501 *via* several integrated physiological mechanisms. Melanin accumulation is positively
502 correlated with cell wall rigidity and structural integrity (Langfelder et al. 2003; Moses et al.
503 2006). Thus, melanin accumulation might provide the mechanical support necessary for the
504 overall cell size expansion, characteristic of titan cells. Furthermore, literature suggests a
505 correlation between melanization and increased cell diameter, indicating a possible role for
506 melanin in supporting cell size growth in *C. neoformans*. (Baker et al. 2024). Previous studies
507 have shown that melanin acts as an antioxidant when *C. neoformans* encounters the host
508 environment, effectively scavenging excessive ROS to maintain cellular redox homeostasis
509 (Zaragoza 2019).. While, endogenous reactive oxygen species (ROS) are known to induce
510 endoreduplication and polyploidy that are required for titanization (Altamirano et al. 2021;

García-Barbazán et al. 2024), excessive ROS accumulation that likely occurs in melanin deficient strains, can be cytotoxic or trigger pleiotropic inhibitory effects. Hence, maintenance of optimum ROS levels would be an important factor for titan cell formation. By scavenging excessive ROS, melanin may act as a redox buffer and maintain the ROS levels within the threshold that is optimal for titan cell formation. A recent study shows that deletion of *gsh2*, a gene encoding for glutathione synthetase, a key enzyme involved in redox homeostasis of *C. neoformans*, attenuates titan cell formation further strengthening the aforesaid hypothesis (Black et al. 2024). While the cAMP-PKA pathway is recognized as a master regulator of capsule expansion, melanin biosynthesis, and titan cell formation in *C. neoformans*, the functional interdependency among these three virulence factors remains poorly defined. Recent studies have indicated a competitive relationship between melanin and the capsule, in capsule-inducing media, wherein melanin deposition within the cell wall negatively impacts capsule expansion by sequestering shared cellular resources (Baker et al. 2024). In contrast to this observation, our findings indicate a synergistic relationship between capsule and melanin during titanization. Specifically, melanin biosynthesis, along with capsule formation (Hommel et al. 2018) appears to promote titan cell formation, in standard *in vitro* titanization conditions. This variation suggests that the regulation of these virulence factors differ depending on the environmental stimuli. Under titan cell-inducing conditions, the cells may metabolically rewire and reallocate its resources to simultaneously promote the biosynthesis of both capsule and melanin to support this dramatic morphological transition. Deciphering the precise molecular mechanisms underlying this complex crosstalk between capsule, melanin and titanization requires further investigation.

In conclusion, our study establishes glycolysis as a critical metabolic pathway that modulates titan cell formation in *C. neoformans* through the regulation of the cAMP-PKA signalling (Fig. 6). Additionally, we also demonstrate that, melanin, a well-characterized virulence factor of *C. neoformans*, is critical for titan cell formation, underscoring its important role in *C. neoformans* pathogenesis. These findings provide new insights into the metabolic basis of morphogenetic transitions in *C. neoformans* and highlight the connections between central carbon metabolism and pathogenesis. Understanding these metabolic requirements not only advances our fundamental knowledge of *C. neoformans* biology but also reveals potential targets for therapeutic intervention against this opportunistic pathogen.

Materials and Methods

Strains and Media:

All strains used in this study are listed in Table 1. All experiments were performed using *Cryptococcus neoformans* var. grubii, serotype A, H99 wild-type, and its derivatives. All strains used in this study were generously provided by Dr. Joeseph Heitman, Duke University, USA. Yeast Peptone (YP) (1% (w/v) yeast extract and 2% (w/v) peptone) medium supplemented with glycerol was used for cryo-preservation of strains at -80 °C. All the strains were recovered at 30 °C on YPD agar plates (1% (w/v) yeast extract, 2% (w/v) peptone, 2% (w/v) glucose and 2% (w/v) agar).

YPD broth containing 1% (w/v) yeast extract, 2% (w/v) peptone and 2% (w/v) glucose was used for the overnight growth of the cultures. Overnight cultures of various strains were grown in YPD broth and incubated at 30 °C with continuous shaking at 200 Rotations Per Minute

558 (RPM). Titan Cell Medium (TCM) containing 5% (w/v) SDA (Sabouraud), 5% (v/v) FBS (Fetal
559 Bovine Serum), 15μM Sodium Azide and 50mM MOPS was used for all *in vitro* titan cell
560 assays.
561
562 **Table 1: *C. neoformans* Strains Used in This Study**

Strain	Genotype	References
Wild-type	*C. neofrormans* var. Grubii, serotype A, H99	(Perfect et al. 1993)
*pyk1*Δ	*C. neofrormans* var. Grubii, serotype A, *pyk1*Δ*::NEO,* (MPC31)	(Price et al. 2011)
*hxk2*Δ	*C. neofrormans* var. Grubii, serotype A, *hxk2*Δ*::NAT,* (AI110)	(Price et al. 2011)
*pyk1*Δ *+ PYK1*	*C. neofrormans* var. Grubii, serotype A, *pyk1::NEO PYK1-NAT (MPC36)*	(Price et al. 2011)
*hxk2*Δ *+ HXK2*	*C. neofrormans* var. Grubii, serotype A, *hxk2::NAT HXK2-NEO, (AI118)*	(Price et al. 2011)
*lac2*Δ	*C. neofrormans var. Grubii, serotype A, lac2*Δ*:: NEO (RPC27)*	(Pukkila-Worley et al. 2005)
*lac2*Δ *+ LAC2*	*C. neofrormans var. Grubii, serotype A, MATα lac2::neo pGPD-LAC2*	(Pukkila-Worley et al. 2005)
*lac1*Δ*lac2*Δ	*C. neofrormans var. Grubii, serotype A, lac1*Δ*:: NAT/ lac2*Δ*:: NEO*	(Pukkila-Worley et al. 2005)

563
564 ## *In Vitro* Titan Cell Assay:
565 For *in vitro* titan cell inducing assays, overnight grown cultures of different *C. neoformans*
566 strains (listed in Table 1) were inoculated in TCM at a cell density of 10^6 CFU per ml. For titan
567 cell inducing assays with glycolysis inhibitors, cultures were grown in TCM at cell density of
568 10^6 CFU per ml with 0.025% (w/v) of 2-Deoxy-D-Glucose (2DG) and 0.5% (w/v) of sodium
569 citrate for 72 hours at 37 °C under 5% CO_2.
570
571 For cAMP add-back assays, wild-type and knockout strains of *C. neoformans* were cultured
572 in TCM at cell density of 10^6 CFU per ml in the presence and absence of 10mM cAMP for 72
573 hours at 37 °C under 5% CO_2. Following 72 hours of incubation, cells were fixed and imaged
574 using Zeiss Apotome microscope. Cell diameter was measured using Zen 2.3 software and
575 titan cell quantification was done (>400 cells per sample). Titan cell percentage was calculated
576 as a ratio of cells with cell body diameter of ≥10μm to total number of cells. Statistical analysis
577 was performed using unpaired t-test with GraphPad Prism (v9.0). Error bars represent the
578 Standard Error of the Mean (SEM). All statistical comparison was based on a minimum of
579 three independent biological replicates.
580
581 ## Capsule Visualization and Analysis:
582 For visualization and analysis of capsule thickness, overnight grown cultures of different
583 *C. neoformans* strains (listed in Table 1) were inoculated in TCM at cell density of 10^6 CFU
584 per ml for 72 hours at 37 °C under 5% CO_2. Following 72 hours of incubation, cells were fixed
585 and stained using India ink. Samples were imaged using Zeiss Apotome microscope. Capsule
586 thickness was measured using Zen 2.3 software (150 cells each sample). Statistical analysis
587 was performed using unpaired t-test with GraphPad Prism (v9.0). Error bars represent the

588 Standard Error of the Mean (SEM). All statistical comparison was based on a minimum of
589 three independent biological replicates.
590
591 **Intracellular cAMP Measurement Assay:**
592 Overnight grown cultures of wild-type and glycolysis mutants *hxk2*Δ and *pyk1*Δ were
593 inoculated in TCM or YPD and grown at 37 °C under shaking conditions. Cells were harvested
594 at mid-log phase (YPD) or after 24 hours (TCM) washed twice with sterile 1X PBS and 10^4
595 cells from each strain were used for cAMP measurement assay using cAMP-Glo assay kit
596 (#V1501 - Promega), as per the manufacturer's instructions. Statistical analysis was
597 performed using unpaired t-test with GraphPad Prism (v9.0). Error bars represent the
598 Standard Error of the Mean (SEM). All statistical comparison was based on a minimum of
599 three independent biological replicates.
600
601 **Cell Viability Assay:**
602 To study the effect of glycolysis inhibitors (2DG and NaCi) on general growth, the overnight
603 culture of wild-type, grown in YPD, was inoculated into TCM at a cell density of 10^6 CFU per
604 ml with and without 2DG (0.025%) or sodium citrate (0.5%) and incubated at 37 °C under 5%
605 CO_2 for 72 hours. After incubation, cells were washed twice with sterile 1X PBS and plated on
606 YPD Agar plates (1% (w/v) yeast extract, 2% (w/v) peptone, 2% (w/v) glucose, 2% (w/v) agar)
607 and incubated for 48 hours at 30 °C.
608
609 For glycolysis mutants, the overnight cultures of glycolysis mutants (*hxk2*Δ and *pyk1*Δ) along
610 with the wild-type, was grown in YPD and inoculated into TCM at a cell density of 10^6 CFU per
611 mL and incubated at 37 °C under 5% CO_2 for 72 hours. After incubation, cells were washed
612 twice with sterile 1X PBS and plated on YPD Agar plates and incubated for 48 hours at 30 °C.
613 Post-incubation colonies were counted and calculated to determine the number of colonies
614 per millilitre. Statistical analysis was performed using unpaired t-test with GraphPad Prism
615 (v9.0). Error bars represent the Standard Error of the Mean (SEM). All statistical comparison
616 was based on a minimum of three independent biological replicates.
617
618 **Reverse Transcriptase-Quantitative Polymerase Chain Reaction (RT-qPCR)**
619 **Assay:**
620 Wild-type and knockout strains (listed in Table 1) of *C. neoformans* were cultured in TCM at
621 cell density of 10^6 CFU per ml for 72 hours at 37 °C under 5% CO_2. Total RNA was extracted
622 following 72 hours of incubation using the Ribopure RNA purification kit (yeast) (cat. #AM1926)
623 following the manufacturers instruction. cDNA biosynthesis was done using PrimeScript cDNA
624 biosynthesis kit (cat. #6110A). Primers used for RT-qPCR were designed using PrimeQuest
625 tool from Integrated DNA Technologies (IDT) and the primers used in these experiments are
626 listed in Table 2. RT-qPCR was performed using iTaq Universal SYBR Green Master Mix (cat.
627 #1725121). Actin was used as housekeeping gene for normalization. The results were
628 analysed using the $2^{-\Delta\Delta CT}$ method and Statistical analysis was performed using Two-way
629 ANOVA test with GraphPad Prism (v9.0). Error bars represent the Standard Error of the Mean
630 (SEM). All statistical comparison was based on a minimum of three independent biological
631 replicates.
632
633
634

635 **Table 2: Primers Used in This Study**

Primer name	Description	5' to 3' Sequence
SV775	*C. neoformans cap10* F1	TAACCTCACGGCTGACTCTA
SV776	*C. neoformans cap10* R1	TTACCATCACCTCGCCAATC
SV781	*C. neoformans lac1* F1	GCAACGAGTTCCAGGTGATAG
SV782	*C. neoformans lac1* R1	GGTATCCTTTCTCACAGGGTTG
SV783	*C. neoformans lac2* F1	AGTGTTGCTCTGGACTGTATG
SV784	*C. neoformans lac2* R1	AGGCTCAGCGGTAGTAATAGA
SV795	*C. neoformans* Actin F1	GCAGAACCGAGAGAAGATGAC
SV796	*C. neoformans* Actin R1	CGGAAGCGTAAAGAGAGAGAAC

636
637
638 **Melanin Biosynthesis Assay:**
639 To assess melanin biosynthesis, wild-type and melanin defective strains (listed in Table 1)
640 were cultured in liquid YPD and incubated at 30 °C overnight. Post incubation, cells were
641 washed with 1X PBS and spotted onto melanin inducing medium (L-DOPA medium, 1g L-
642 asparagine, 3g KH2PO4, 0.25g MgSO4, 1mg thiamine, 5µg biotin, and 100mg L-DOPA
643 containing 0.1% glucose). Cells were incubated at 37 °C and were imaged using SZX16 after
644 36 hours.
645
646 **Illustrations:**
647 Figure illustrations were created using Biorender (https://app.biorender.com).
648
649
650
651
652
653
654
655
656
657
658
659
660
661
662
663
664
665
666
667
668
669
670
671

Acknowledgements

We extend our immense gratitude to Dr. Joseph Heitman and Mrs. Anna Floyd-Averette for generously providing the strains used in this study. We would like to thank Dr. Sunil Laxman (BRIC-inStem) for critical reading of our manuscript. We gratefully acknowledge the invaluable support and resources offered by CSIR-Centre for Cellular and Molecular Biology (CCMB) central facilities including Advanced Microscopy and Imaging facility (AMIF). PSP thanks Council of Scientific and Industrial Research (CSIR), India for her research fellowship. SV acknowledges funding from Indian Council of Medical Research (ICMR) (IIRPSG-2024-01-02717), India; Anusandhan National Research Foundation (ANRF) (SRG/2023/000470), India; Council of Scientific & Industrial Research (CSIR) (FTT070505), India; and DBT-Wellcome Trust India Alliance (IA/E/16/1/502996), India.

Author Contributions

Pallavi S Phatak: Investigation; Formal analysis; Visualization; Writing-original draft. **Sudharsan Mathivathanan:** Investigation; Writing-original draft. **Dhrumi Shah:** Investigation; Writing-original draft. **Ishvarya Suresh:** Investigation; Writing-original draft. **Mary Shejo:** Investigation; Writing-original draft. **Santosh Kumar Das :** Investigation; **Sriram Varahan:** Conceptualization; Supervision; Funding acquisition; Investigation; Formal analysis; Visualization; Writing-original draft; Writing-review and editing.

Conflict of Interest

The authors declare that they have no conflict of interests.

References

1. Alspaugh JA, Perfect JR, Heitman J. 1997. Cryptococcus neoformans mating and virulence are regulated by the G- protein α subunit GPA1 and cAMP. Genes Dev. [published online ahead of print]. https://doi.org/10.1101/gad.11.23.3206
2. Altamirano S et al. 2021. The Cyclin Cln1 Controls Polyploid Titan Cell Formation following a Stress-Induced G2 Arrest in Cryptococcus. MBio. [published online ahead of print]. https://doi.org/10.1128/mBio.02509-21
3. Bahn YS et al. 2007. Sensing the environment: Lessons from fungi. Nat Rev Microbiol. [published online ahead of print]. https://doi.org/10.1038/nrmicro1578
4. Baker RP, Liu AZ, Casadevall A. 2024. Cell wall melanin impedes growth of the Cryptococcus neoformans polysaccharide capsule by sequestering calcium. Proc Natl Acad Sci U S A. [published online ahead of print]. https://doi.org/10.1073/pnas.2412534121
5. Black B et al. 2024. Glutathione-mediated redox regulation in Cryptococcus neoformans impacts virulence. Nat Microbiol 2024 98. 9(8):2084–2098 [accessed 2025 Aug 8]. https://www.nature.com/articles/s41564-024-01721-x. https://doi.org/10.1038/s41564-024-01721-x
6. Brown JC, Ballou ER. 2024. Is Cryptococcus neoformans a pleomorphic fungus? Curr Opin Microbiol. 82:102539 [accessed 2025 Jul 31]. https://www.sciencedirect.com/science/article/pii/S1369527424001152. https://doi.org/10.1016/J.MIB.2024.102539
7. Busti S, Coccetti P, Alberghina L, Vanoni M. 2010. Glucose signaling-mediated coordination of cell growth and cell cycle in Saccharomyces Cerevisiae. Sensors. [published online ahead of print]. https://doi.org/10.3390/s100606195
8. Cadart C, Heald R. 2022. Scaling of biosynthesis and metabolism with cell size. Mol Biol Cell. [published online ahead of print]. https://doi.org/10.1091/mbc.E21-12-0627
9. Caza M, Kronstad JW. 2019. The cAMP/protein kinase a pathway regulates virulence and adaptation to host conditions in cryptococcus neoformans. Front Cell Infect Microbiol. [published online ahead of print]. https://doi.org/10.3389/fcimb.2019.00212
10. Chen M et al. 2018. Epidemiology of fungal infections in China. Front Med. [published online ahead of print]. https://doi.org/10.1007/s11684-017-0601-0
11. Choi J, Vogl AW, Kronstad JW. 2012. Regulated expression of cyclic AMP-dependent protein kinase A reveals an influence on cell size and the secretion of virulence factors in Cryptococcus neoformans. Mol Microbiol. [published online ahead of print]. https://doi.org/10.1111/j.1365-2958.2012.08134.x
12. Crabtree JN et al. 2012. Titan cell production enhances the virulence of Cryptococcus neoformans. Infect Immun. [published online ahead of print]. https://doi.org/10.1128/IAI.00507-12
13. Cramer FB, Woodward GE. 1952. 2-Desoxy-D-glucose as an antagonist of glucose in yeast fermentation. J Franklin Inst. [published online ahead of print]. https://doi.org/10.1016/0016-0032(52)90852-1
14. Cramer KL et al. 2006. Transcription factor Nrg1 mediates capsule formation, stress response, and pathogenesis in Cryptococcus neoformans. Eukaryot Cell. [published online ahead of print]. https://doi.org/10.1128/EC.00145-06
15. Cruickshank JG, Cavill R, Jelbert M. 1973. Cryptococcus neoformans of unusual morphology. Appl Microbiol. [published online ahead of print]. https://doi.org/10.1128/aem.25.2.309-312.1973
16. D'Souza CA et al. 2001. Cyclic AMP-Dependent Protein Kinase Controls Virulence of the Fungal Pathogen Cryptococcus neoformans . Mol Cell Biol. [published online ahead of print]. https://doi.org/10.1128/mcb.21.9.3179-3191.2001
17. D'Souza CA, Heitman J. 2001. Conserved cAMP signaling cascades regulate fungal development and virulence. FEMS Microbiol Rev. [published online ahead of print]. https://doi.org/10.1016/S0168-6445(01)00058-4
18. Dambuza IM et al. 2018. The Cryptococcus neoformans Titan cell is an inducible and regulated morphotype underlying pathogenesis. PLoS Pathog. [published online ahead of print]. https://doi.org/10.1371/journal.ppat.1006978
19. Diehl FF, Sapp KM, Vander Heiden MG. 2024. The bidirectional relationship between metabolism and cell cycle control. Trends Cell Biol. [published online ahead of print]. https://doi.org/10.1016/j.tcb.2023.05.012
20. Eisenman HC, Casadevall A. 2012. Synthesis and assembly of fungal melanin. Appl Microbiol Biotechnol. [published online ahead of print]. https://doi.org/10.1007/s00253-011-3777-2
21. Feldmesser M, Kress Y, Casadevall A. 2001. Dynamic changes in the morphology of Cryptococcus neoformans during murine pulmonary infection. Microbiology. [published online ahead of print]. https://doi.org/10.1099/00221287-147-8-2355
22. Fuller KK, Rhodes JC. 2012. Protein kinase A and fungal virulence. Virulence. [published online ahead of print]. https://doi.org/10.4161/viru.19396
23. García-Barbazán I et al. 2016. The formation of titan cells in Cryptococcus neoformans depends on the mouse strain and correlates with induction of Th2-type responses. Cell Microbiol. [published online ahead of print]. https://doi.org/10.1111/cmi.12488
24. García-Barbazán I et al. 2024. Accumulation of endogenous free radicals is required to induce titan-like cell formation in Cryptococcus neoformans. MBio. [published online ahead of print].

https://doi.org/10.1128/mbio.02549-23
25. García-Rodas R, de Oliveira H, Trevijano-Contador N, Zaragoza O. 2019. Cryptococcal titan cells: When yeast cells are all grown up. In: Current Topics in Microbiology and Immunology. https://doi.org/10.1007/82_2018_145
26. Guerra P et al. 2022. TORC1 and PKA activity towards ribosome biogenesis oscillates in synchrony with the budding yeast cell cycle. J Cell Sci. [published online ahead of print]. https://doi.org/10.1242/jcs.260378
27. Hicks JK, D'Souza CA, Cox GM, Heitman J. 2004. Cyclic AMP-Dependent Protein Kinase Catalytic Subunits Have Divergent Roles in Virulence Factor Production in Two Varieties of the Fungal Pathogen Cryptococcus neoformans. Eukaryot Cell. [published online ahead of print]. https://doi.org/10.1128/EC.3.1.14-26.2004
28. Hommel B et al. 2018. Titan cells formation in Cryptococcus neoformans is finely tuned by environmental conditions and modulated by positive and negative genetic regulators. PLoS Pathog. [published online ahead of print]. https://doi.org/10.1371/journal.ppat.1006982
29. Hu G et al. 2007. Transcriptional regulation by protein kinase A in Cryptococcus neoformans. PLoS Pathog. [published online ahead of print]. https://doi.org/10.1371/journal.ppat.0030042
30. Idnurm A, Giles SS, Perfect JR, Heitman J. 2007. Peroxisome function regulates growth on glucose in the basidiomycete fungus Cryptococcus neoformans. Eukaryot Cell. [published online ahead of print]. https://doi.org/10.1128/EC.00214-06
31. Kalucka J et al. 2015. Metabolic control of the cell cycle. Cell Cycle. [published online ahead of print]. https://doi.org/10.1080/15384101.2015.1090068
32. Kierans SJ, Taylor CT. 2024. Glycolysis: A multifaceted metabolic pathway and signaling hub. J Biol Chem. 300(11) [accessed 2025 Aug 1]. https://pubmed.ncbi.nlm.nih.gov/39442619/. https://doi.org/10.1016/j.jbc.2024.107906
33. Langfelder K et al. 2003. Biosynthesis of fungal melanins and their importance for human pathogenic fungi. Fungal Genet Biol. [published online ahead of print]. https://doi.org/10.1016/S1087-1845(02)00526-1
34. Leadsham JE, Gourlay CW. 2010. CAMP/PKA signaling balances respiratory activity with mitochondria dependent apoptosis via transcriptional regulation. BMC Cell Biol. [published online ahead of print]. https://doi.org/10.1186/1471-2121-11-92
35. Mahmood F ; et al. 2024. Roles of Different Signaling Pathways in Cryptococcus neoformans Virulence. J Fungi 2024, Vol 10, Page 786. 10(11):786 [accessed 2025 Aug 1]. https://www.mdpi.com/2309-608X/10/11/786/htm. https://doi.org/10.3390/JOF10110786
36. Moses DN et al. 2006. Role of melanin in mechanical properties of Glycera jaws. Acta Biomater. [published online ahead of print]. https://doi.org/10.1016/j.actbio.2006.05.002
37. Mukaremera L et al. 2018. Titan cell production in Cryptococcus neoformans reshapes the cell wall and capsule composition during infection. Cell Surf. [published online ahead of print]. https://doi.org/10.1016/j.tcsw.2017.12.001
38. Nosanchuk JD, Casadevall A. 2003. The contribution of melanin to microbial pathogenesis. Cell Microbiol. [published online ahead of print]. https://doi.org/10.1046/j.1462-5814.2003.00268.x
39. O'Meara TR, Andrew Alspaugh J. 2012. The Cryptococcus neoformans capsule: A sword and a shield. Clin Microbiol Rev. [published online ahead of print]. https://doi.org/10.1128/CMR.00001-12
40. Okagaki LH et al. 2010. Cryptococcal cell morphology affects host cell interactions and pathogenicity. PLoS Pathog. [published online ahead of print]. https://doi.org/10.1371/journal.ppat.1000953
41. Okagaki LH et al. 2011. Cryptococcal Titan Cell Formation Is Regulated by G-Protein Signaling in Response to Multiple Stimuli ∇. Eukaryot Cell. [published online ahead of print]. https://doi.org/10.1128/EC.05179-11
42. Okagaki LH, Nielsen K. 2012. Titan cells confer protection from phagocytosis in Cryptococcus neoformans infections. Eukaryot Cell. [published online ahead of print]. https://doi.org/10.1128/EC.00121-12
43. Peeters K et al. 2017. Fructose-1,6-bisphosphate couples glycolytic flux to activation of Ras. Nat Commun. [published online ahead of print]. https://doi.org/10.1038/s41467-017-01019-z
44. Perfect JR et al. 1993. Karyotyping of Cryptococcus neoformans as an epidemiological tool. J Clin Microbiol. [published online ahead of print]. https://doi.org/10.1128/jcm.31.12.3305-3309.1993
45. Price MS et al. 2011. Cryptococcus neoformans requires a functional glycolytic pathway for disease but not persistence in the host. MBio. 2(3) [accessed 2025 Aug 1]. /doi/pdf/10.1128/mbio.00103-11?download=true. https://doi.org/10.1128/MBIO.00103-11/SUPPL_FILE/MBIO.00103-11-S1.PDF
46. Pukkila-Worley R et al. 2005. Transcriptional network of multiple capsule and melanin genes governed by the Cryptococcus neoformans cyclic AMP cascade. Eukaryot Cell. [published online ahead of print]. https://doi.org/10.1128/EC.4.1.190-201.2005
47. Pukkila-Worley R, Alspaugh JA. 2004. Cyclic AMP signaling in Cryptococcus neoformans. FEMS Yeast Res. [published online ahead of print]. https://doi.org/10.1016/S1567-1356(03)00241-1
48. Rajasingham R et al. 2017. Global burden of disease of HIV-associated cryptococcal meningitis: an updated analysis. Lancet Infect Dis. 17(8):873–881 [accessed 2025 Aug 4]. https://pubmed.ncbi.nlm.nih.gov/28483415/. https://doi.org/10.1016/S1473-3099(17)30243-8
49. Sachla AJ, Helmann JD. 2021. Resource sharing between central metabolism and cell envelope synthesis. Curr Opin Microbiol. [published online ahead of print]. https://doi.org/10.1016/j.mib.2021.01.015

50. Shah D et al. 2026. Glycolysis-dependent Sulfur Metabolism Orchestrates Morphological Plasticity and Virulence in Fungi. Elife. 14 [accessed 2026 Feb 3]. https://elifesciences.org/reviewed-preprints/109075. https://doi.org/10.7554/eLife.109075.2
51. Stempinski PR, Gerbig GR, Greengo SD, Casadevall A. 2023. Last but not yeast-The many forms of Cryptococcus neoformans. PLoS Pathog. [published online ahead of print]. https://doi.org/10.1371/journal.ppat.1011048
52. Trevijano-Contador N et al. 2018. Cryptococcus neoformans can form titan-like cells in vitro in response to multiple signals. PLoS Pathog. [published online ahead of print]. https://doi.org/10.1371/journal.ppat.1007007
53. Xue C, Bahn YS, Cox GM, Heitman J. 2006. G protein-coupled receptor Gpr4 senses amino acids and activates the cAMP-PKA pathway in Cryptococcus neoformans. Mol Biol Cell. [published online ahead of print]. https://doi.org/10.1091/mbc.E05-07-0699
54. Xue Y, Batlle M, Hirsch JP. 1998. GPR1 encodes a putative G protein-coupled receptor that associates with the Gpa2p G(α) subunit and functions in a Ras-independent pathway. EMBO J. 17(7):1996–2007 [accessed 2025 Aug 7]. /doi/pdf/10.1093/emboj/17.7.1996?download=true. https://doi.org/10.1093/EMBOJ/17.7.1996
55. Yoboue ED et al. 2012. cAMP-induced mitochondrial compartment biogenesis: Role of glutathione redox state. J Biol Chem. [published online ahead of print]. https://doi.org/10.1074/jbc.M111.302786
56. Yoshino M, Murakami K. 1982. AMP deaminase as a control system of glycolysis in yeast. Mechanism of the inhibition of glycolysis by fatty acid and citrate. J Biol Chem. [published online ahead of print]. https://doi.org/10.1016/s0021-9258(18)33871-7
57. Yu PL, Rollins JA. 2022. The cAMP-dependent protein kinase A pathway perturbs autophagy and plays important roles in development and virulence of Sclerotinia sclerotiorum. Fungal Biol. [published online ahead of print]. https://doi.org/10.1016/j.funbio.2021.09.004
58. Yu S et al. 2025. The protein phosphatase 2C domain contributes to the pathobiological function of adenylyl cyclase in Cryptococcus neoformans bioRxiv. 2025.12.10.693573 http://biorxiv.org/content/early/2025/12/11/2025.12.10.693573.abstract. https://doi.org/10.64898/2025.12.10.693573
59. Yuan HX, Xiong Y, Guan KL. 2013. Nutrient Sensing, Metabolism, and Cell Growth Control. Mol Cell. [published online ahead of print]. https://doi.org/10.1016/j.molcel.2013.01.019
60. Zaragoza O et al. 2009. Chapter 4 The Capsule of the Fungal Pathogen Cryptococcus neoformans. Adv Appl Microbiol. [published online ahead of print]. https://doi.org/10.1016/S0065-2164(09)01204-0
61. Zaragoza O et al. 2010. Fungal cell gigantism during mammalian infection. PLoS Pathog. [published online ahead of print]. https://doi.org/10.1371/journal.ppat.1000945
62. Zaragoza O. 2019. Basic principles of the virulence of Cryptococcus. Virulence. [published online ahead of print]. https://doi.org/10.1080/21505594.2019.1614383
63. Zaragoza O, Nielsen K. 2013. Titan cells in Cryptococcus neoformans: Cells with a giant impact. Curr Opin Microbiol. [published online ahead of print]. https://doi.org/10.1016/j.mib.2013.03.006
64. Zhao Y et al. 2023. Cryptococcus neoformans, a global threat to human health. Infect Dis Poverty. [published online ahead of print]. https://doi.org/10.1186/s40249-023-01073-4
65. Zhou X, Ballou ER. 2018. The Cryptococcus neoformans Titan Cell: From In Vivo Phenomenon to In Vitro Model. Curr Clin Microbiol Reports. [published online ahead of print]. https://doi.org/10.1007/s40588-018-0107-9

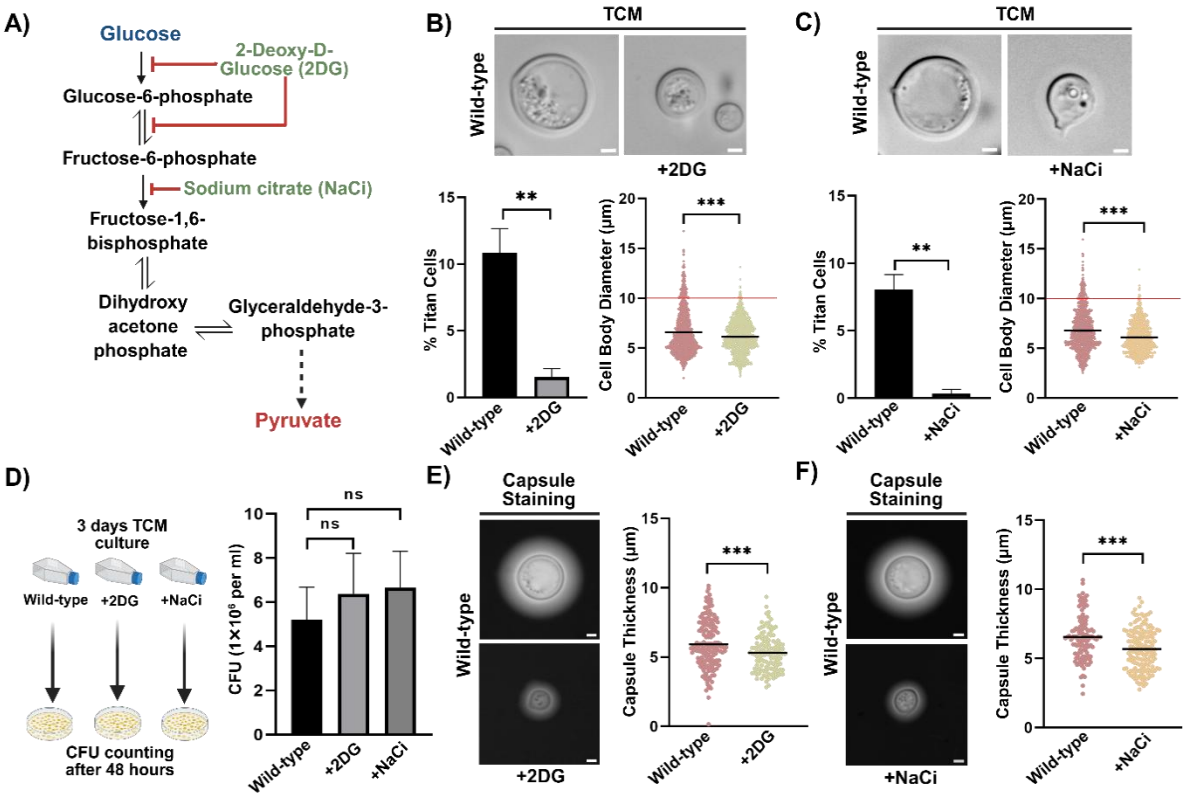

Fig. 1. Effect of Glycolysis Inhibitors on Titan Cell Formation in *C. neoformans.*

(A) Schematic overview of glycolysis and its inhibition by glycolysis inhibitors (2-Deoxy-D-Glucose (2DG) and sodium citrate (NaCi)). (B) Wild-type strain was cultured in Titan Cell Medium (TCM) with and without inhibitor (2DG (0.025%)) at 37 °C with 5% CO_2 for 72 hours. Cells were fixed and imaged using Zeiss Apotome microscope. Percentage of titan cells was quantified as a ratio of cells with diameter ≥10µm to total number of cells. Cell diameter was measured using Zen 2.3 software. Threshold for cell body diameter of titan cells is indicated by the red line. More than 400 cells were counted for each condition. Statistical analysis was done using unpaired t-test, ***($p<0.001$) and **($p<0.01$). Error bars represent SEM Scale bars represents 2µm. (C) Wild-type strain was cultured in TCM with and without inhibitor (NaCi (0.5%)) at 37 °C with 5% CO_2 for 72 hours. Cells were fixed and imaged using Zeiss Apotome microscope. Percentage of titan cells was quantified as a ratio of cells with diameter ≥10µm to total number of cells. Cell diameter was measured using Zen 2.3 software. Threshold for cell body diameter of titan cells is indicated by the red line. More than 400 cells were counted for each condition. Statistical analysis was done using unpaired t-test, ***($p<0.001$) and **($p<0.01$). Error bars represent SEM Scale bars represents 2µm. (D) Colony Forming Units (CFU) analysis was performed to monitor overall viability of wild-type strain in TCM, +2DG and +NaCi conditions. Wild-type cultures were grown under TCM conditions with and without glycolysis inhibitors for 72 hours and plated on YPD plates and incubated at 30 °C for 48 hours. CFU quantification was done post incubation. Statistical analysis was done using unpaired t-test, ns (non-significant). Error bars represent SEM. (E) For capsule visualization, wild-type strain was cultured in TCM with and without 2DG at 37 °C with 5% CO_2 for 72 hours, cells were stained with India ink and imaging was done using Zeiss Apotome microscope. Capsule thickness was measured using Zen 2.3 software. Approximately 150 cells were counted for each condition. Statistical analysis was done using unpaired t-test, ***($p<0.001$). Error bars represent SEM Scale bars represents 2µm. (F) For capsule visualization, wild-type strain was cultured in TCM with and without NaCi at 37 °C with 5% CO_2 for 72 hours, cells were stained with India ink and imaging was done using Zeiss Apotome microscope. Capsule thickness was measured using Zen 2.3 software. Approximately 150 cells were counted for each condition. Statistical analysis was done using unpaired t-test, ***($p<0.001$). Error bars represent SEM. Scale bars represents 2µm. This figure was created using Biorender.

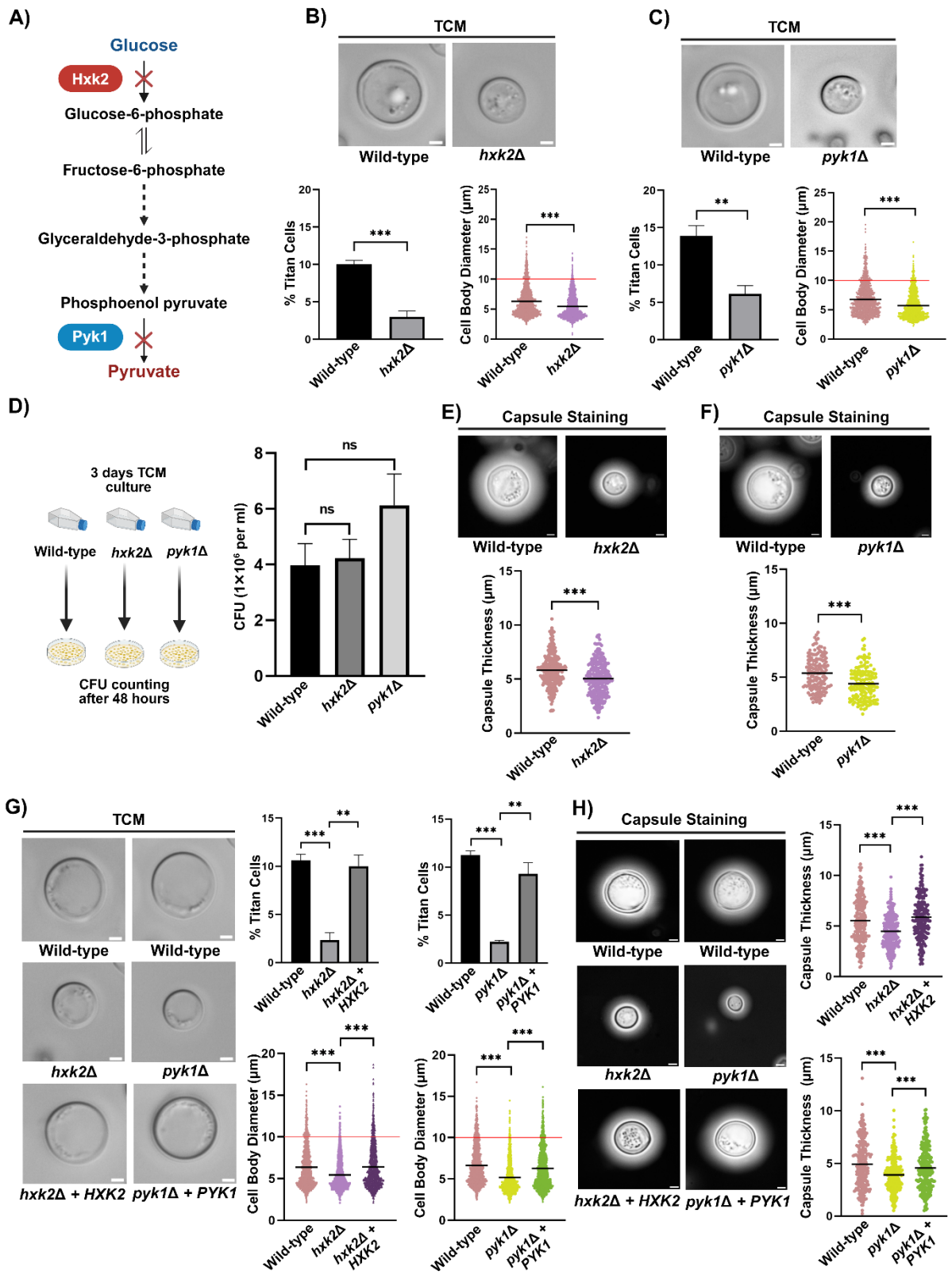

Fig. 2. Genetic Perturbation of Glycolysis Attenuates Titan Cell Formation in *C. neoformans.*

Overview of glycolysis pathway showing targeted gene deletions. (B) Wild-type and *hxk2Δ* strains were cultured in Titan Cell Medium (TCM) at 37 °C with 5% CO_2 for 72 hours. Cells were fixed and imaged using Zeiss Apotome microscope. Percentage of titan cells was quantified as a ratio of cells with diameter ≥10µm to total number of cells.

Cell diameter was measured using Zen 2.3 software. Threshold for cell body diameter of titan cells is indicated by the red line. More than 400 cells were counted for each condition. Statistical analysis was done using unpaired t-test, ***($p<0.001$). Error bars represent SEM. Scale bars represents 2μm. (C) Wild-type and *pyk1Δ* strains were cultured in TCM at 37 °C with 5% CO_2 for 72 hours. Cells were fixed and imaged using Zeiss Apotome microscope. Percentage of titan cells was quantified as a ratio of cells with diameter ≥10μm to total number of cells. Cell diameter was measured using Zen 2.3 software. Threshold for cell body diameter of titan cells is indicated by the red line. More than 400 cells were counted for each condition. Statistical analysis was done using unpaired t-test, ***($p<0.001$) **($p<0.01$). Error bars represent SEM. Scale bars represents 2μm. (D) CFU analysis was performed to monitor overall viability of wild-type and knockout strains including *hxk2Δ*, and *pyk1Δ* in TCM. Wild-type, *hxk2Δ*, and *pyk1Δ* strains were grown under TCM conditions for 72 hours and plated on YPD plates and incubated at 30 °C for 48 hours. CFU quantification was done post incubation. Statistical analysis was done using unpaired t-test, ns (non-significant). Error bars represent SEM. (E) For capsule visualization, wild-type, and *hxk2Δ* strains were cultured in TCM at 37 °C with 5% CO_2 for 72 hours, cells were stained with India ink and imaging was done using Zeiss Apotome microscope. Capsule thickness was measured using Zen 2.3 software. Approximately 150 cells were counted for each condition. Statistical analysis was done using unpaired t-test, ***($p<0.001$). Error bars represent SEM. Scale bars represents 2μm. (F) For capsule visualization, wild-type and *pyk1Δ* strains were cultured in TCM at 37 °C with 5% CO_2 for 72 hours, cells were stained with India ink and imaging was done using Zeiss Apotome microscope. Capsule thickness was measured using Zen 2.3 software. Approximately 150 cells were counted for each condition. Statistical analysis was done using unpaired t-test, ***($p<0.001$). Error bars represent SEM. Scale bars represents 2μm. (G) Wild-type, *hxk2Δ, pyk1Δ, hxk2Δ + HXK2* and *pyk1Δ + PYK1* strains were cultured in TCM at 37 °C with 5% CO_2 for 72 hours. Cells were fixed and imaged using Zeiss Apotome microscope. Percentage of titan cells was quantified as a ratio of cells with diameter ≥10μm to total number of cells. Cell diameter was measured using Zen 2.3 software. Threshold for cell body diameter of titan cells is indicated by the red line. More than 400 cells were counted for each condition. Statistical analysis was done using unpaired t-test, ***($p<0.001$) **($p<0.01$). Error bars represent SEM Scale bars represents 2μm. (H) For capsule visualization, wild-type, *hxk2Δ, pyk1Δ, hxk2Δ + HXK2* and *pyk1Δ + PYK1* strains were cultured in TCM at 37 °C with 5% CO_2 for 72 hours, cells were stained with India Ink and imaging was done using Zeiss Apotome microscope. Capsule thickness was measured using Zen 2.3 software. Approximately 150 cells were counted for each condition. Statistical analysis was done using unpaired t-test, ***($p<0.001$). Error bars represent SEM. Scale bars represents 2μm. This figure was created using Biorender.

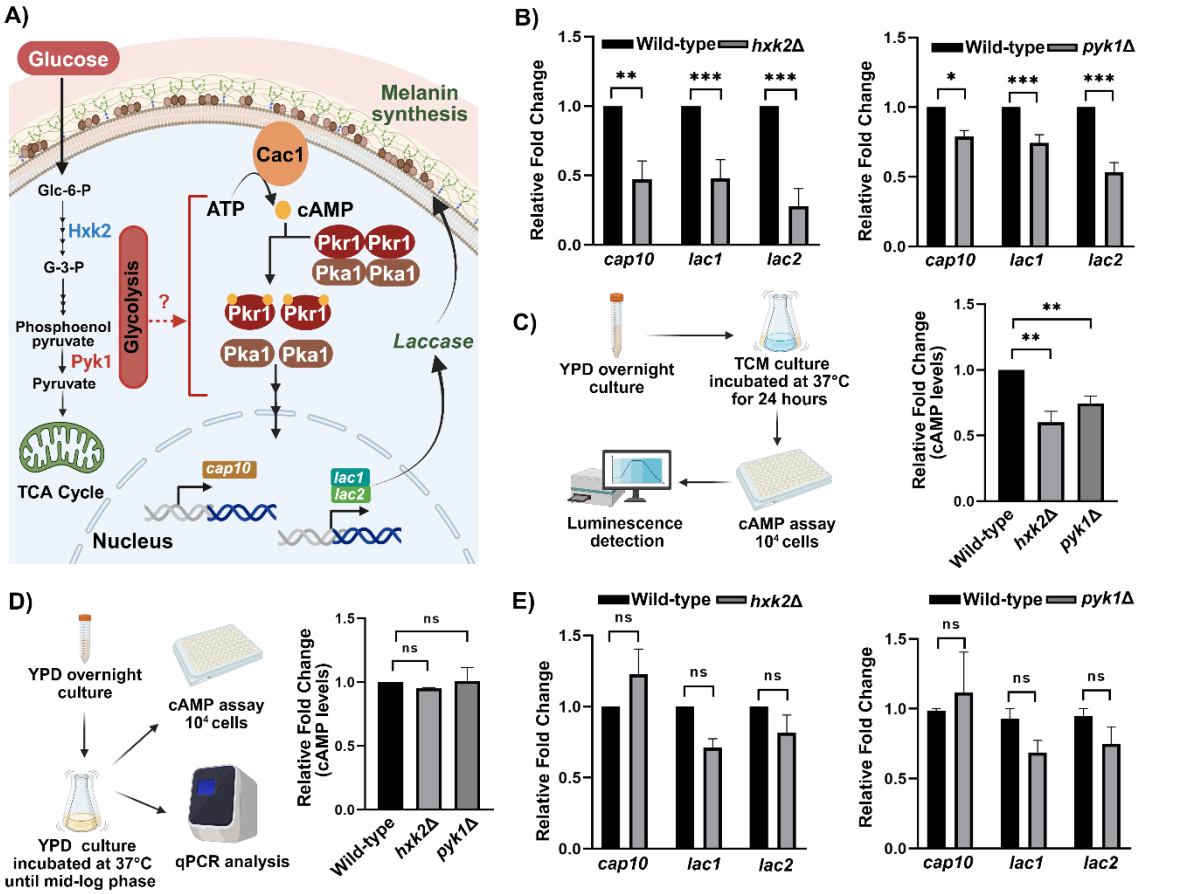

Fig. 3. Active Glycolysis is Critical for cAMP-PKA Signalling in Titan Cell Inducing Conditions.

(A) Overview of cAMP-PKA pathway regulating the expression of key genes involved in capsule formation and melanin biosynthesis. (B) Wild-type, *hxk2*Δ and *pyk1*Δ strains were cultured in Titan Cell Medium (TCM) at 37 °C with 5% CO_2 for 72 hours. Total RNA was extracted after 72 hours and comparative RT-qPCR was performed. Statistical analysis was done using Two-Way ANOVA, ***($p<0.001$), **($p<0.01$), *($p<0.05$). Error bars represent SEM. (C) Schematic for intracellular cAMP measurement assay. Wild-type strain, *hxk2*Δ, and *pyk1*Δ strains were cultured in TCM at 37 °C in shaking conditions for 24 hours. cAMP measurement assay was performed using cAMP-Glo assay kit. Statistical analysis was done using unpaired t-test, **($p<0.01$). Error bars represent SEM, (D) Schematic for intracellular cAMP measurement assay and RT-qPCR analysis for YPD grown cultures. Wild-type strain, *hxk2*Δ, and *pyk1*Δ strains were cultured in YPD medium at 37 °C in shaking conditions and cells were collected at mid-log phase. cAMP measurement assay was performed using cAMP-Glo assay kit. Statistical analysis was done using unpaired t-test, ns (non-significant). Error bars represent SEM, (E) Wild-type strain, *hxk2*Δ, and *pyk1*Δ strains were cultured in YPD medium at 37 °C in shaking conditions and cells were collected at mid-log phase. Total RNA was extracted after 72 hours and comparative RT-qPCR was performed. Statistical analysis was done using Two-Way ANOVA, ns (non-significant). Error bars represent SEM. This figure was created using Biorender.

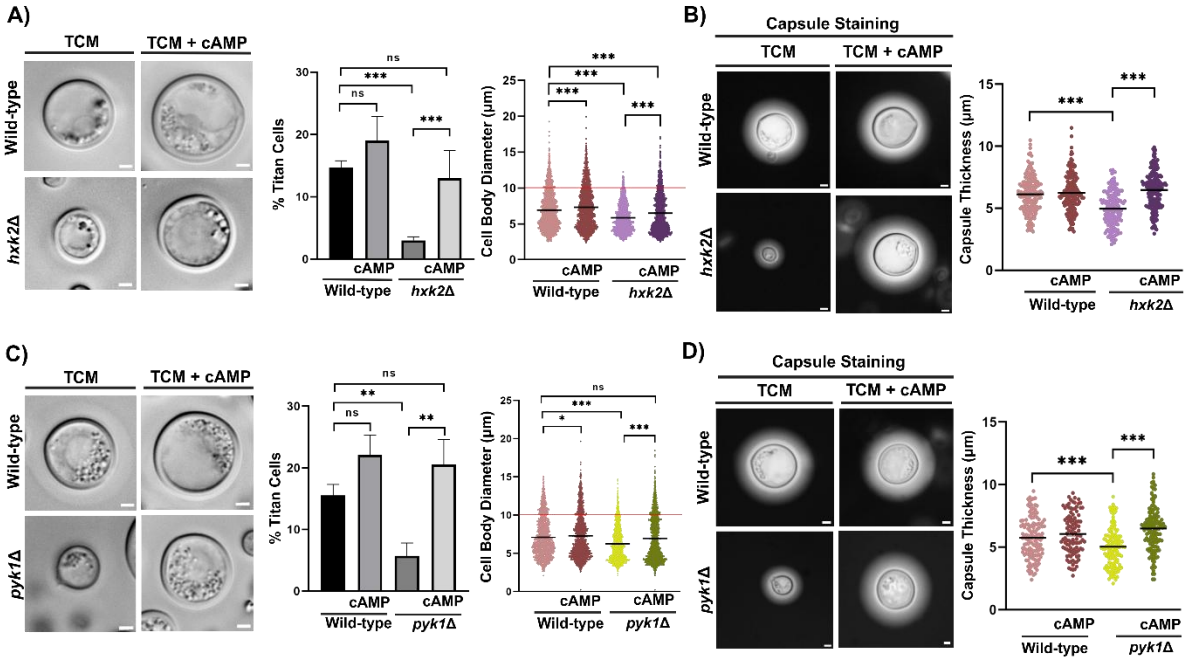

1020
1021 **Fig. 4. Glycolysis Orchestrates Titan Cell Formation in a cAMP-PKA Dependent**
1022 **Manner.**
1023 (A) Wild-type and *hxk2*Δ strains were cultured in Titan Cell Medium (TCM) in the presence and absence of cAMP
1024 (10mM) at 37 °C with 5% CO_2 for 72 hours. Cells were fixed and imaged using Zeiss Apotome microscope.
1025 Percentage of titan cells was quantified as a ratio of cells with diameter ≥10µm to total number of cells. Cell diameter
1026 was measured using Zen 2.3 software. Threshold for cell body diameter of titan cells is indicated by the red line.
1027 More than 400 cells were counted for each condition. Statistical analysis was done using unpaired t-test,
1028 ***($p<0.001$), and ns (non-significant). Error bars represent SEM. Scale bar represents 2µm. (B) For capsule
1029 visualization, wild-type and *hxk2*Δ strains were cultured in TCM in the presence and absence of cAMP (10mM) at
1030 37 °C with 5% CO_2 for 72 hours, cells were stained with India ink and imaging was done using Zeiss Apotome
1031 microscope. Capsule thickness was measured using Zen 2.3 software. Approximately 150 cells were counted for
1032 each condition. Statistical analysis was done using unpaired t-test, ***($p<0.001$). Error bars represent SEM Scale
1033 bar represents 2µm. (C) Wild-type and *pyk1*Δ strains were cultured in TCM in the presence and absence of cAMP
1034 (10mM) at 37 °C with 5% CO_2 for 72 hours. Cells were fixed and imaged using Zeiss Apotome microscope.
1035 Percentage of titan cells was quantified as a ratio of cells with diameter ≥10µm to total number of cells. Cell diameter
1036 was measured using Zen 2.3 software. Threshold for cell body diameter of titan cells is indicated by the red line.
1037 More than 400 cells were counted for each condition. Statistical analysis was done using unpaired t-test,
1038 ***($p<0.001$), **($p<0.01$), *($p<0.05$) and ns (non-significant). Error bars represent SEM. Scale bar represents 2µm.
1039 (D) For capsule visualization, wild-type and *pyk1*Δ strains were cultured in TCM in the presence and absence of
1040 cAMP (10mM) at 37 °C with 5% CO_2 for 72 hours, cells were stained with India Ink and imaging was done using
1041 Zeiss Apotome microscope. Capsule thickness was measured using Zen 2.3 software. Approximately 150 cells
1042 were counted for each condition. Statistical analysis was done using unpaired t-test, ***($p<0.001$). Error bars
1043 represent SEM. Scale bar represents 2µm. This figure was created using Biorender.
1044

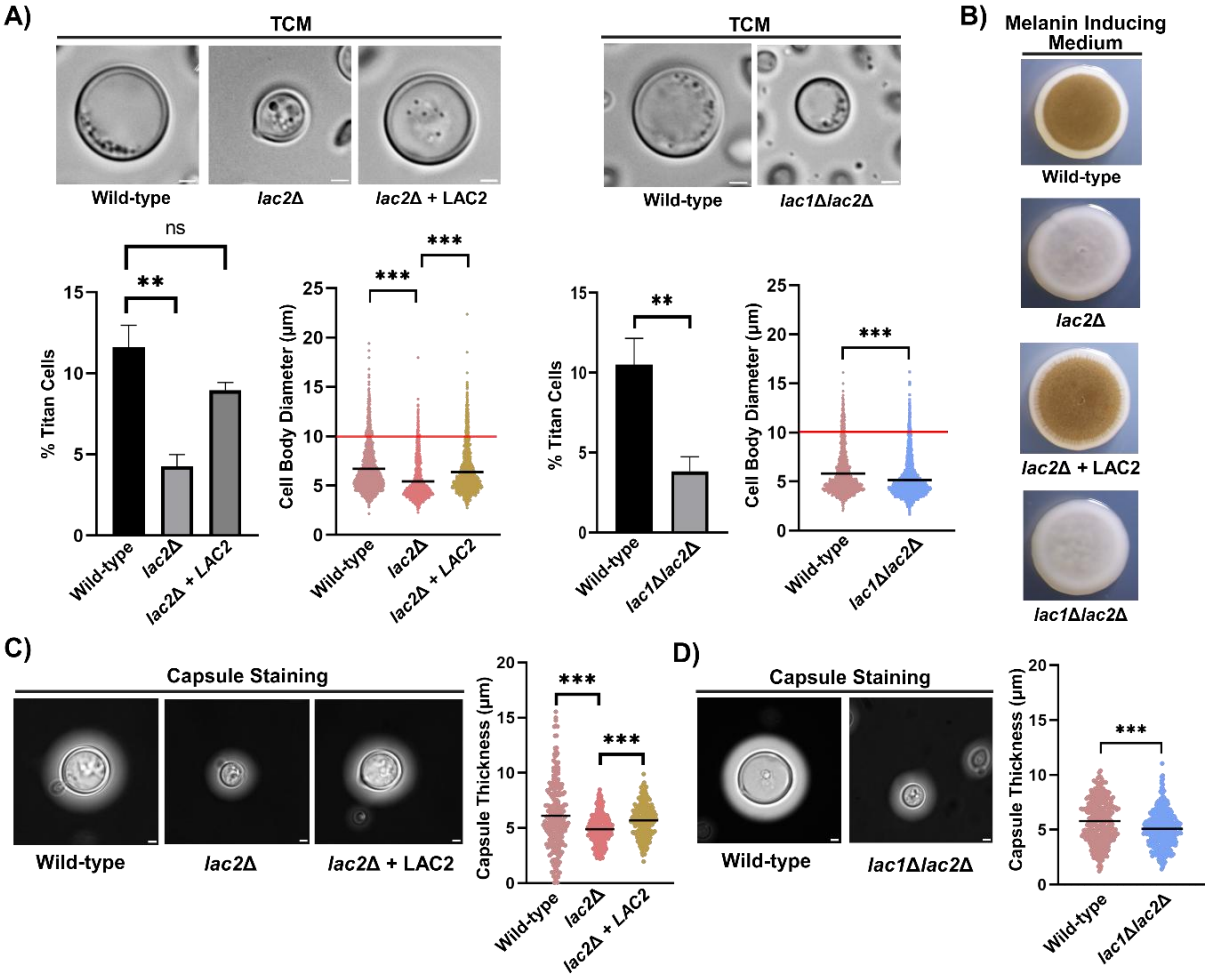

Fig. 5. Melanin Biosynthesis is Critical for Titan Cell Formation in *C. neoformans.*
(A) Wild-type, *lac2*Δ, *lac2*Δ + LAC2 and *lac1*Δ*lac2*Δ strains were cultured in Titan Cell Medium (TCM) at 37 °C with 5% CO_2 for 72 hours. Cells were fixed and imaged using Zeiss Apotome microscope. Percentage of Titan cells was quantified as a ratio of cells with diameter ≥10µm to total number of cells. Cell diameter was measured using Zen 2.3 software. Threshold for cell body diameter of titan cells is indicated by red line. More than 200 cells were counted for each condition. Statistical analysis was done using unpaired t-test, ***($p<0.001$), **($p<0.01$) and ns (non-significant). Error bars represent SEM. Scale bar represents 2µm. (B) Wild-type, *lac2*Δ, *lac2*Δ + LAC2 and *lac1*Δ*lac2*Δ strains were spotted on melanin inducing medium and incubated at 37 °C for 36 hours. After incubation the colonies were imaged using SZX16 microscope. (C) For capsule visualization, wild-type, *lac2*Δ and *lac2*Δ + LAC2 strains were cultured in TCM at 37 °C with 5% CO_2 for 72 hours, cells were stained with India ink and imaging was done using Zeiss Apotome microscope. Capsule thickness was measured using Zen 2.3 software. Approximately 150 cells were counted for each condition. Statistical analysis was done using unpaired t-test, ***($p<0.001$). Scale bar represents 2µm. (D) For capsule visualization, wild-type and *lac1*Δ*lac2*Δ strains were cultured in TCM at 37 °C with 5% CO_2 for 72 hours, cells were stained with India ink and imaging was done using Zeiss Apotome microscope. Capsule thickness was measured using Zen 2.3 software. Approximately 150 cells were counted for each condition. Statistical analysis was done using unpaired t-test, Error bars represent SEM, ***($p<0.001$). Scale bar represents 2µm. This figure was created using Biorender.

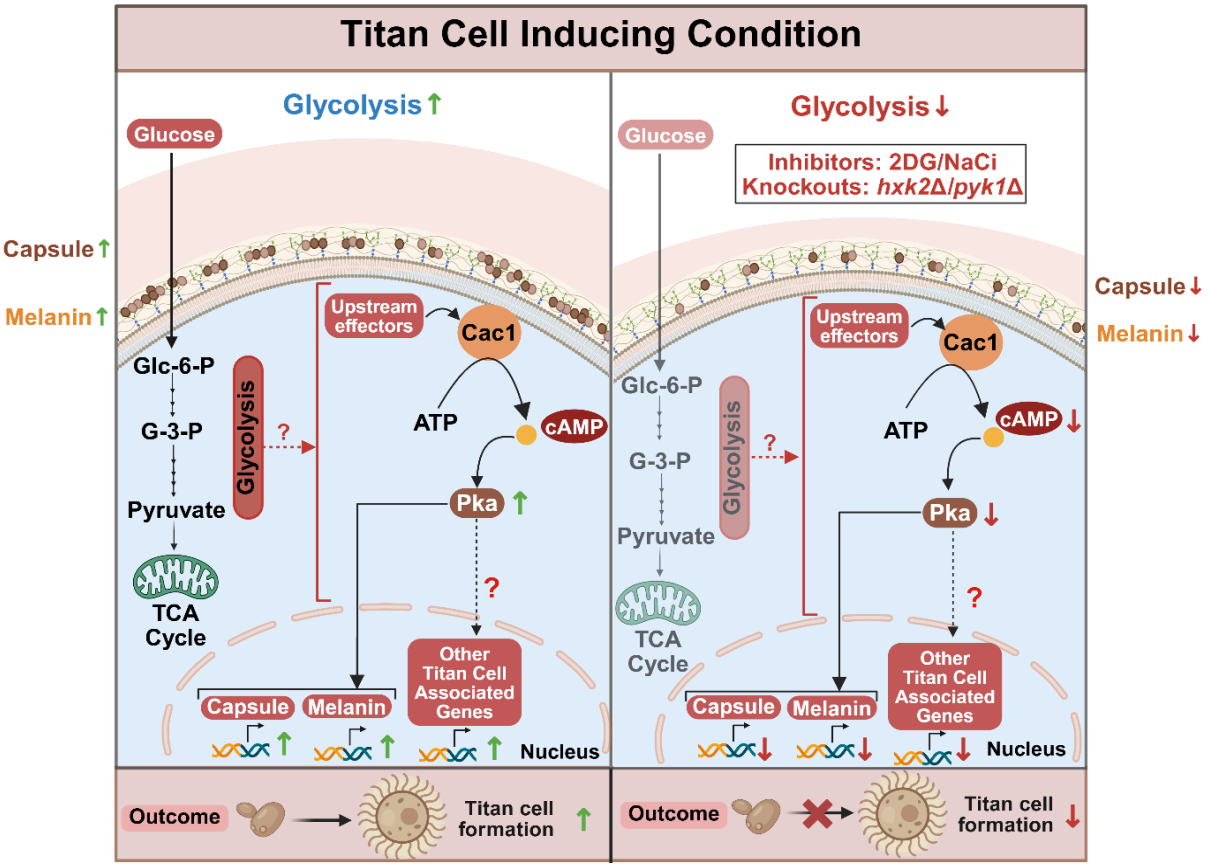

Fig. 6. A Conserved Metabolic Network Regulates Titan Cell Formation in *C. neoformans*.

Active glycolysis plays a critical role in the regulation of the cAMP-PKA signalling pathway which in turn affects the regulation of virulence factors of *C. neoformans* including capsule formation, melanin biosynthesis and titan cell formation. Perturbation of glycolysis either through glycolysis inhibitors (2DG and NaCi) or pertinent knockout strains (*hxk2*Δ and *pyk1*Δ), leads to a downregulation of cAMP-PKA pathway. The suppression of cAMP-PKA pathway impairs capsule formation and melanin biosynthesis, ultimately resulting in attenuated titan cell formation. This figure was created using Biorender.

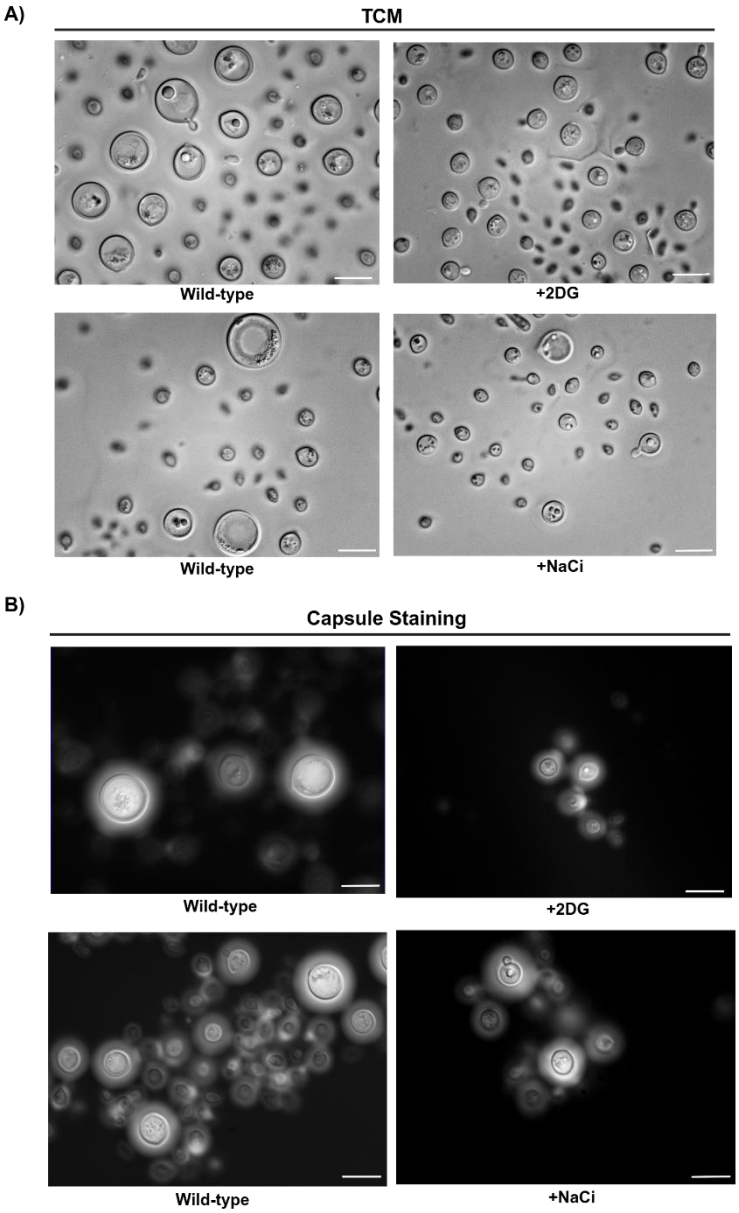

Fig. S1. Wider Field Images of TCM Grown *C. neoformans* Treated with Glycolysis Inhibitors.

(A) Representative wider field images of TCM grown wild-type cultures, in presence and absence of sub-inhibitory concentration of glycolysis inhibitors (2DG and NaCi). Scale bar represents 10μm. (B) Representative wider field images of India ink staining for capsule visualization of TCM grown wild-type cultures, in presence and absence of sub-inhibitory concentration of glycolysis inhibitors (2DG and NaCi). Scale bar represents 10μm. This figure was created using Biorender.

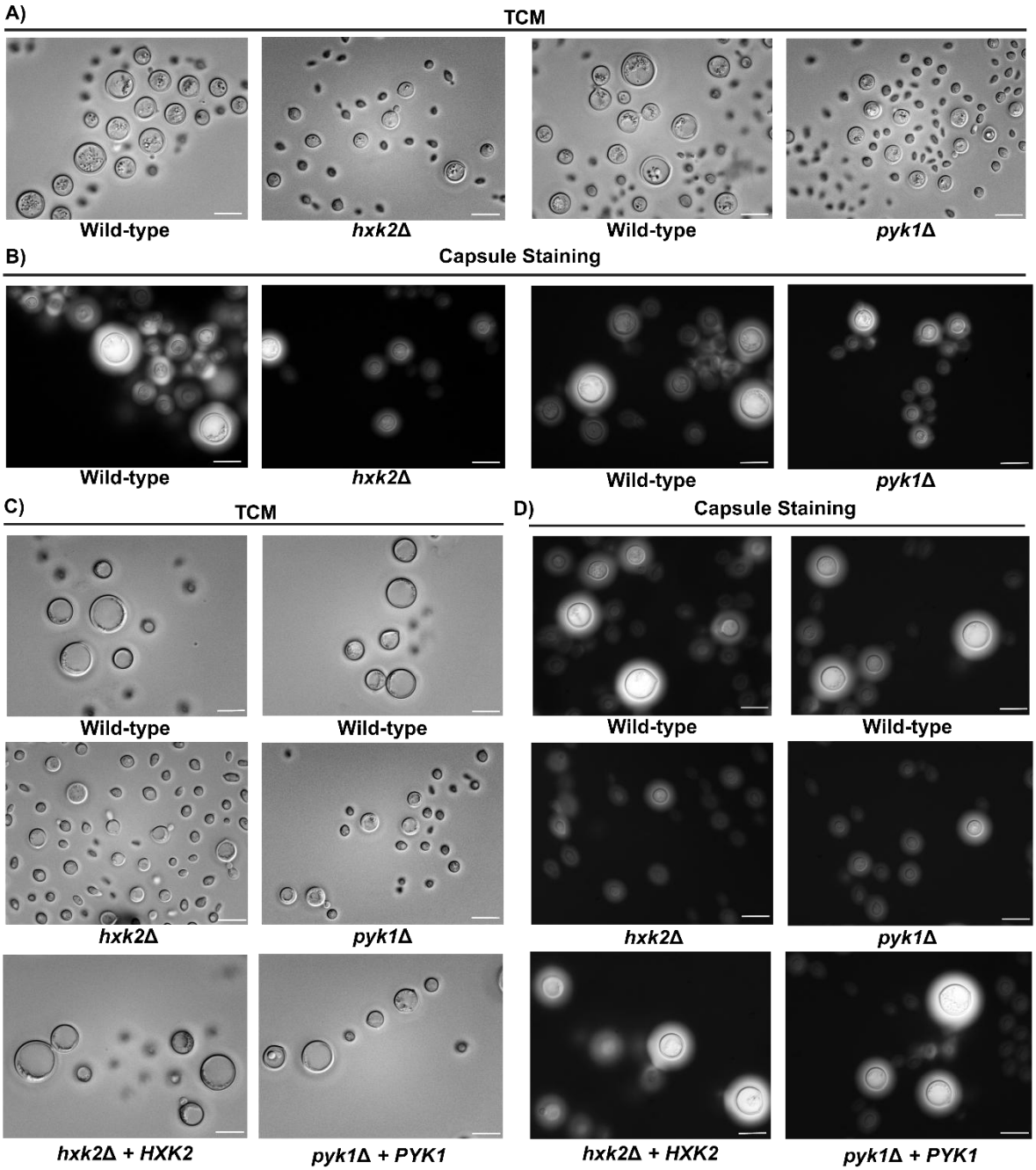

Fig. S2. Wider Field Images of TCM Grown Wild-type and Glycolysis Mutants of *C. neoformans*.

(A) Representative wider field images of wild-type, and glycolysis mutants including *hxk2*Δ, *pyk1*Δ grown under titan cell inducing conditions. Scale bar represents 10µm. (B) Representative wider field images of India ink staining for capsule visualization of wild-type, and glycolysis mutants including *hxk2*Δ, *pyk1*Δ grown under titan cell inducing conditions. Scale bar represents 10µm. (C) Representative wider field images of wild-type, *hxk2*Δ, *pyk1*Δ, *hxk2Δ + HXK2* and *pyk1Δ + PYK1* strains grown under titan cell inducing conditions. Scale bar represents 10µm. (D) Representative wider field images of India ink staining for capsule visualization of wild-type, *hxk2*Δ, *pyk1*Δ, *hxk2Δ + HXK2* and *pyk1Δ + PYK1* strains grown under titan cell inducing conditions. Scale bar represents 10µm. This figure was created using Biorender.

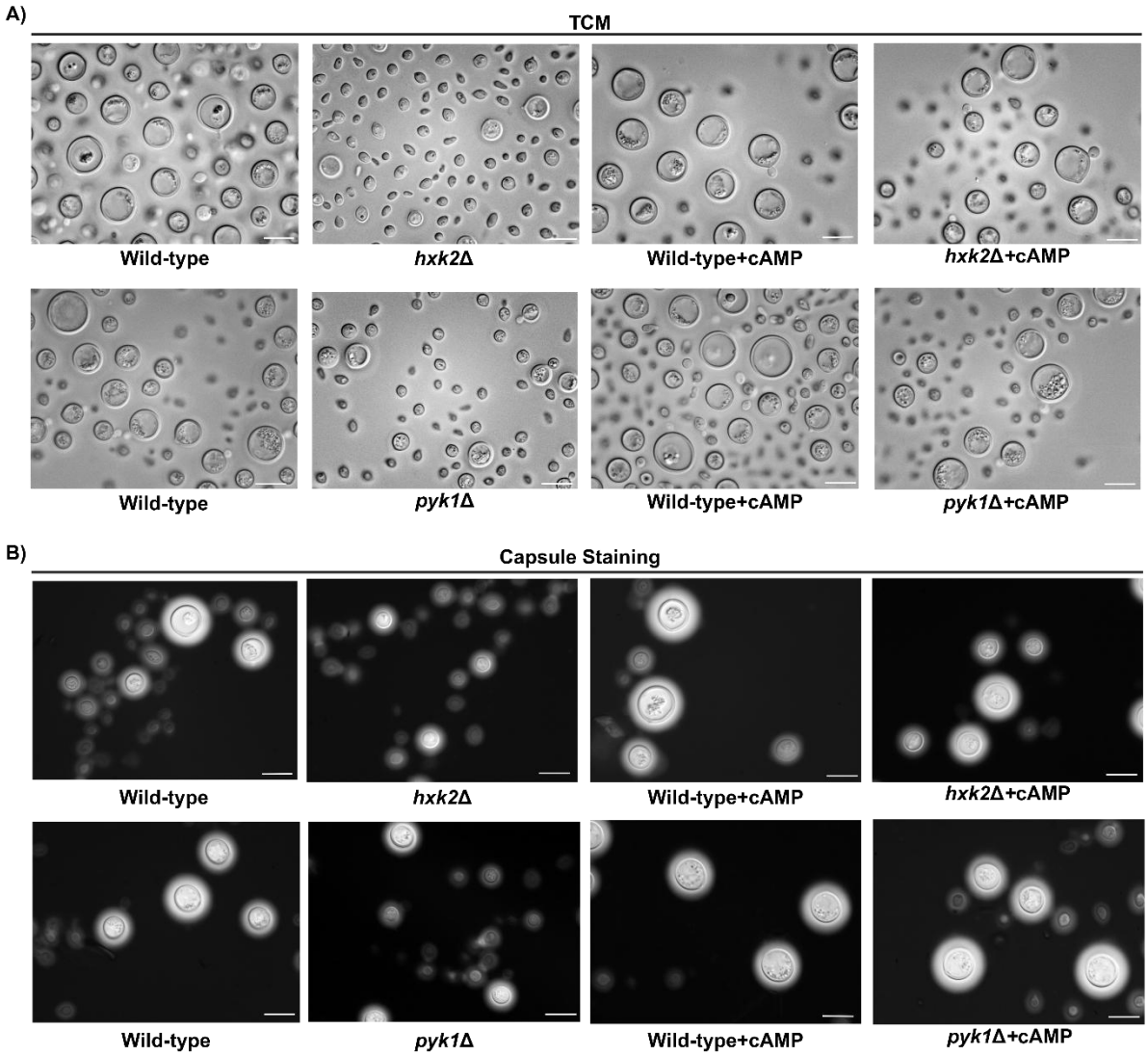

Fig. S3. Wider Field Images of cAMP Add-back Assay for Glycolysis Mutants of *C. neoformans* in TCM.

(A) Representative wider field images of wild-type, and glycolysis mutants including *hxk2*Δ and *pyk1*Δ grown under titan cell inducing conditions with and without exogenous supplementation of cAMP. Scale bar represents 10μm. (B) Representative wider field images of India ink staining for capsule visualization of wild-type, and glycolysis mutants including *hxk2*Δ and *pyk1*Δ grown under titan cell inducing conditions with and without exogenous supplementation of cAMP. Scale bar represents 10μm. This figure was created using Biorender.

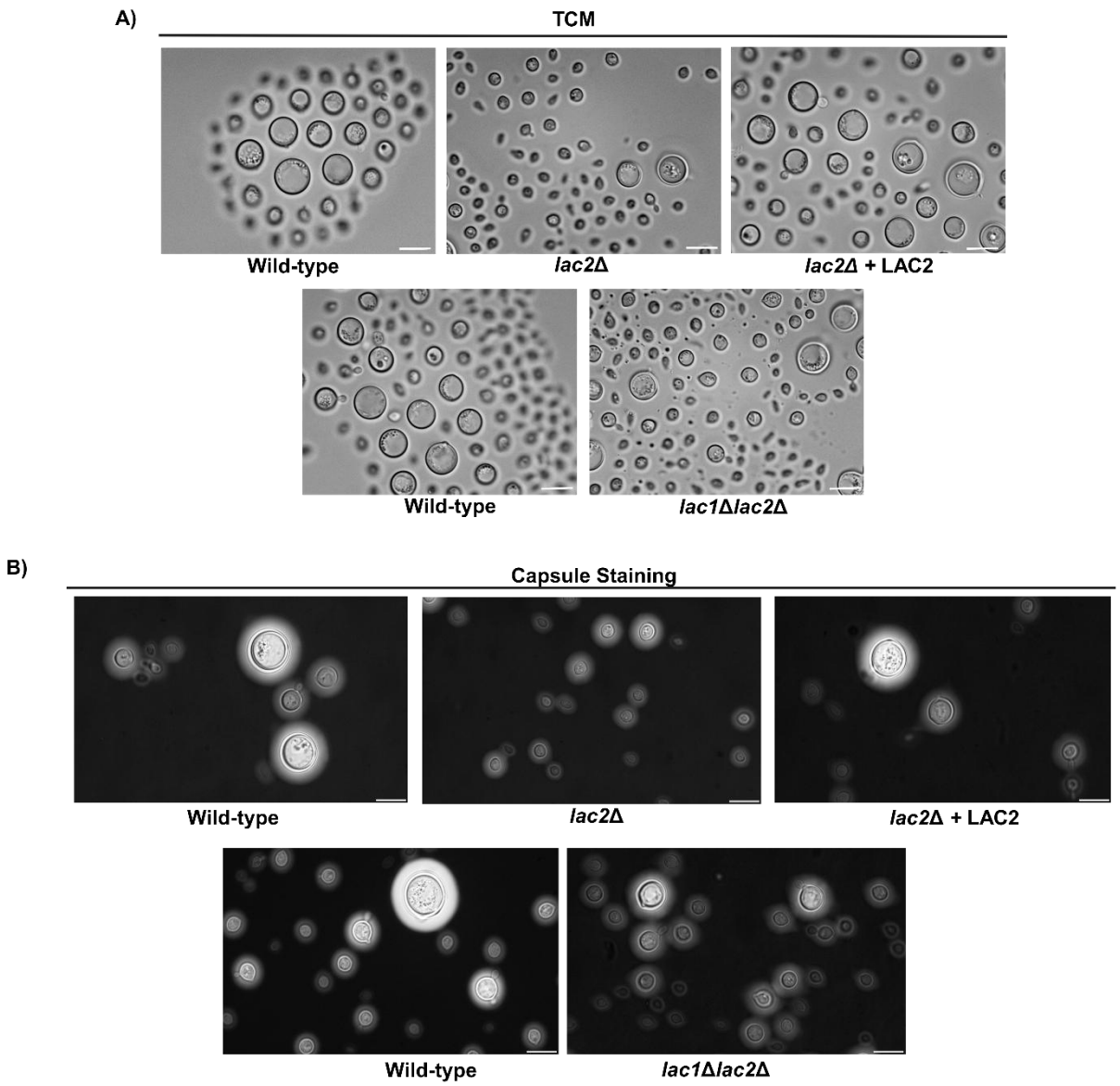

1151
1152 **Fig. S4. Wider Field Images of TCM Grown Wild-Type and Melanin Deficient Mutants of**
1153 ***C. neoformans* in TCM.**
1154 (A) Representative wider field images of wild-type, *lac2*Δ, *lac2*Δ + *LAC2* and *lac1*Δ*lac2*Δ strains grown under titan
1155 cell inducing conditions. Scale bar represents 10μm. (B) Representative wider field images of India ink staining for
1156 capsule visualization of wild-type, *lac2*Δ, *lac2*Δ + *LAC2* and *lac1*Δ*lac2*Δ strains grown under titan cell inducing
1157 conditions. Scale bar represents 10μm. This figure was created using Biorender.
1158